12-2021

To a More Sustainable Construction Method for Electrically Conductive Heated Pavement Systems

Mohammad Anis
The University of Texas Rio Grande Valley

TO A MORE SUSTAINABLE CONSTRUCTION METHOD FOR ELECTRICALLY CONDUCTIVE HEATED PAVEMENT SYSTEMS

A Thesis

by

MOHAMMAD ANIS

Submitted to the Graduate College of
The University of Texas Rio Grande Valley
In partial fulfillment of the requirements for the degree of

MASTER OF SCIENCE

Major Subject: Civil Engineering

The University of Texas Rio Grande Valley

December 2021

TO A MORE SUSTAINABLE CONSTRUCTION METHOD FOR ELECTRICALLY CONDUCTIVE HEATED PAVEMENT SYSTEMS

A Thesis

by

MOHAMMAD ANIS

COMMITTEE MEMBERS

Dr. Mohamed Abdel-Raheem
Chair of Committee

Dr. Philip Park
Committee Member

Dr. Thang Pham
Committee Member

Dr. Nazmul Islam
Committee Member

December 2021

ABSTRACT

Anis, Mohammad, TO A More Sustainable Construction Method For Electrically Conductive Pavement. Master of Science in Engineering (MSE), December, 2021, 80 pp., 13 Tables, 34 Figures, 139 References.

Snow and ice damage to the pavement in the United States, particularly in colder regions, costs the US economy millions of dollars each year. Conventional methods for keeping snow off roads after heavy snowfall are judged prohibitively expensive. As a result, an alternative solution is required to reduce costs while also improving pavement resiliency. An electrically heated pavement system (EHPS) has been regarded as a viable alternative to older approaches in recent years. The majority of earlier research concentrated on improving the conductivity characteristics of paving materials. On the other hand, this study takes a different approach by focusing on the construction method rather than changing the properties of materials. This study focuses on the construction method, followed by using two ELECTRICALLY CONDUCTIVE COMPOSITE materials, such as WPU-GP and EP-GP, and coated on the PCC substrate using the parallel stripe method. The results show that the construction approach utilizing WPU-GP produced 22.5%, and EP-GP produced 17.5% GP validated the concept of sustainable EHPS construction. Furthermore, increasing the coating thickness improves the heating effect of the pavement surface, and resistive heating performance improves steadily with higher voltage application, although lower coating spacing demonstrated better surface heating performance.

DEDICATION

I dedicate my work to my mother, Ayesha Begum; my father, Abdur Rahim; and my three siblings. Thanks to the almighty for helping me and guiding me through the difficult times. Without my supervisor, family, and friends' constant support and help, my journey here at UTRGV would not have been possible.

ACKNOWLEDGMENT

I would like to acknowledge my supervisor, Dr. Mohamed Abdel-Raheem, for his outstanding guidance and support. His knowledge and expertise in the advanced construction method and his ongoing mentorship have helped me overcome all the difficulties I faced during this master's program. I am delighted that I got the opportunity to work in the Construction Research Field under his supervision. Besides, I am very thankful to Dr. Jungseok Ho, Dr. Jong-Min Kim, Dr. Philip Park, and Dr. Thang Pham. I want to thank Abdullah Al-Masum, Apu Deb, Aminur Rashid Chowdury, Farzana Tasnim, Md Riyad Hossain, Nizamul Nibir, Sharmin Emu , Zisan Mashfiqur, and Saumik Skaib for making my journey smooth at the earlier stage. I am also thankful to my colleague KIM Iqbal for his continuous encouragement and support.

TABLE OF CONTENTS

Page

LIST OF TABLES

Page

LIST OF FIGURES

Page

CHAPTER I

INTRODUCTION

The transportation system has been continuously developing since ancient times, which helped the rapid growth of urbanization, so transportation safety is the main issue of people. That depends not only on the passenger, driver, vehicles, characteristics of the highways but also overall climatic condition. Moisture, ice, or snow on the pavement are critical factors of natural climatic conditions, which lead to brake failure and cause accidents. This chapter introduces an overview of this study, defines the problem statement, describes research objectives, and finally provides an outline of the thesis.

1.1 General Overview

Most northern US pavements are vulnerable to below-freezing temperatures and heavy precipitation during the winter season. With the presence of ice and snow on the pavement, this state makes the roads potentially risky for vehicles to use since it reduces the friction between the pavement and the tires [1]. Due to this scenario, traffic flow is halted or experiences delays, resulting in lower-traffic volume on US roadways during the cold season. It is possible to suffer substantial economic losses as well as a large number of accidents. Every year, millions of dollars are spent by authorities to keep roadways free of ice or snow, allowing traffic to flow without interruption. Among the most commonly used methods to keep off snow and ice accumulation on roads are the application of deicing chemicals [2], the use of snowplows [3], and mechanical snow removal; however, these are associated with being labor-intensive,

sluggish, and expensive [4], as well as the possibility of causing pavement [4]–[10]. In addition, typical deicing methods are inefficient in inclement weather. At temperatures below -10°C, most deicing salts, for example, have been demonstrated to be useless in melting snow [11]. While successful deicing chemicals like calcium chloride work well below (-17°C), they increase the danger of damage to the rigid pavement from steel corrosion [12], and machinery may struggle to work in freezing conditions [12]. For years, implemented numerous sustainable methods for removing snow off roadways, eventually moving toward employing clean energy technologies rather than traditional methods, which have a negative environmental impact and are a source of a large amount of pollution [13], [14]. In recent years, a heated pavement system (EHPS) has been deemed as a viable alternative to traditional methods for keeping snow off pavements, as it is ecologically friendly, cost-effective, long-lasting, and simple to maintain [15], etc. Existing technologies of EHPS, including hydronic heated pavement systems [16], [17], infrared heating method [18], embedded resistive heating elements [19], carbon fiber grills [17], superhydrophobic coating [20]–[22], electrically conductive concrete [12], [23]–[26], and electrically conductive coating [27]. Among deicing practices, electrically conductive pavement is likely the most efficient snow removal technology. Even though this system has shown promising results, its greater capital costs have made them impractical to utilize in the real world [28]. As a result, developing a more sustainable deicing method was necessary, which has become a significant problem in recent years.

1.2 Problem and Objectives

The problem identified from previous studies concentrated mainly on the effectiveness of melting snow electrically or through the heat without taking into account the cost, environment,

or society of the approach used. This study is being conducted to fill in the gaps and propose a new construction method for electrically conductive pavement that is deemed cost-effective.

1.3 Conceptualization

The idea behind this research is inspired by the thermal conductive paint used in the car windshields for evaporating the water vapor. A similar methodology applied in this research, which results in constructing a new method for deicing pavements containing electrically conductive composite stripes, is shown in Figure 1. This method is regarded as a more sustainable construction option for safely and securely removing ice snow from the pavement in terms of cost-effectiveness, minimum impact on pavement, and environmental friendliness. However, in order for this strategy to make sense, it must address various issues, such as material conductivity, durability, the longevity of applied coating, and concerns regarding ride smoothness.

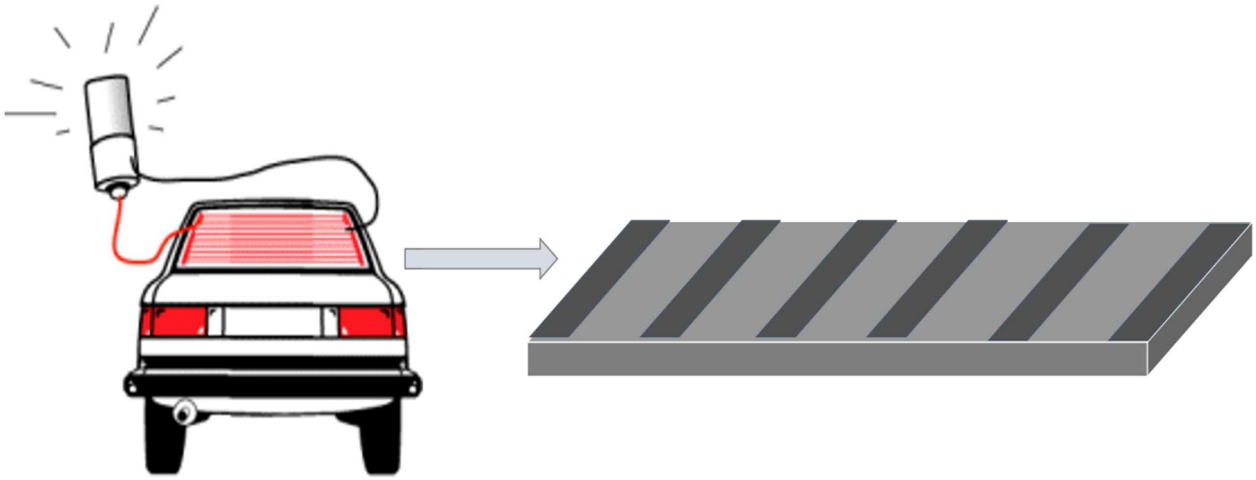

Figure 1: The conception of a new construction method of an electrically conductive pavement.

1.4 Methodology

Following literature reviews, the illustrated concept and methodology proceed to identify suitable materials for the application surface of the pavement. Durable materials were considered

in this process because the abrasion of rider tires may damage the applied materials. In order to prevent and assure smoothness of the ride, a smooth layer of PCC has been put on top of the coated surface to ensure smoothness of the surface during the pavement construction. Figure 2 depicts the steps involved in this methodology.

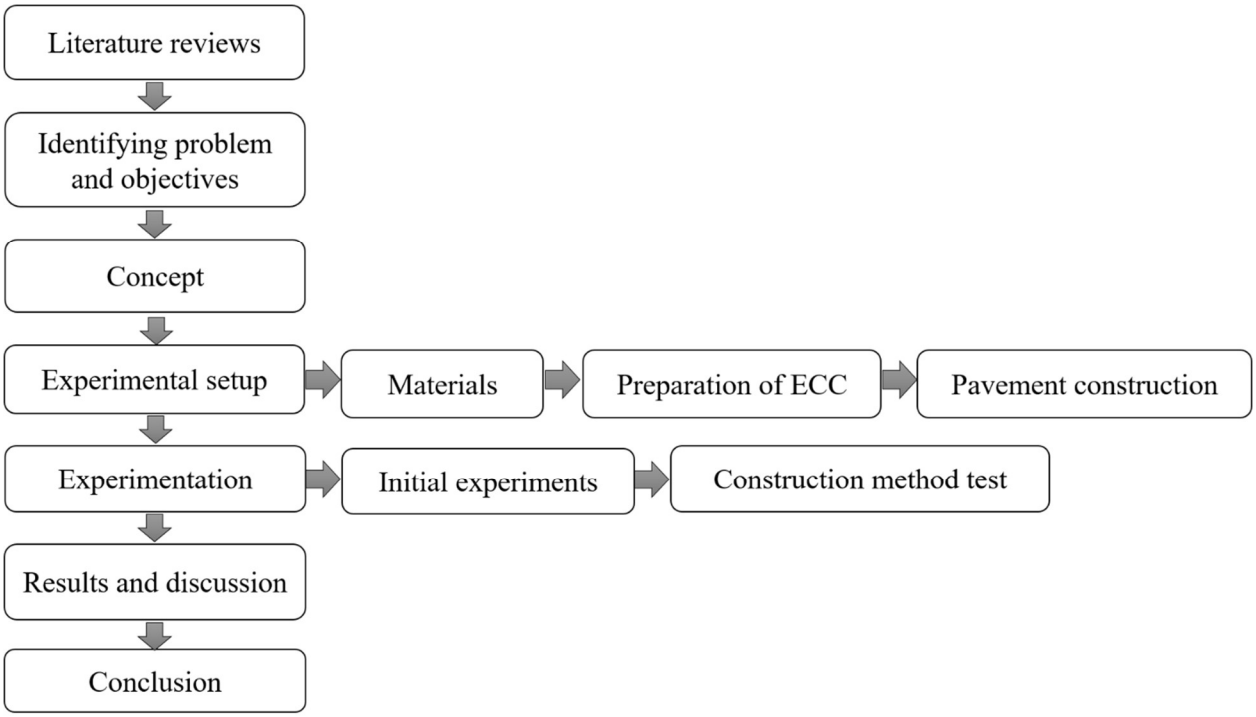

Figure 2: The methodology of this study.

1.5 Thesis Organization

This thesis consists of five sections, and their contents are as follows:

Section 1 gives the introduction of the study topic. The problems and objectives of the research are stated in the section.

Section 2 presents a comprehensive literature review related to the study. Previous studies focusing on different snow removal methods are briefly discussed in the section. Since the research focuses on proposing a construction method that is performing better than the electrically conductive concrete and it was discussed broadly in this section.

Section 3 included the ingredients needed to prepare the coating, the steps that follow the coating mixing procedure, and the pavement construction methods for the investigating specimens.

Section 4 was divided into two tasks: first, determining the surface resistivity and heating capacity distribution of the applied materials, and second, determining the efficiency of the construction method.

Section 5 gives conclusions from the study and illuminates the future research that needs to be done.

CHAPTER II

LITERATURE REVIEW

Ice has been removed successfully from the pavement by introducing a set of techniques, such as thermal, chemical, and mechanical treatment. During the cold season, roads undergo routine maintenance procedures using snow-melting chemical substances or machinery, which are the foremost ways for deicing and anti-icing [2]. That leads to hindrances and requires considerable labor, besides chemical substances and machinery, which is undoubtedly labor-intensive and sluggish. The usage of chemical compounds, for example, sodium chloride, can cause undesirable conditions on environment, function, and structure [29]; damage to concrete pavement such as rebar deterioration, pavement erosion, and disturbance of the soil eco-friendly settings [30], [31], even though sodium chloride is thought to be the most economical product for deicing [2];. Simultaneously, mechanical tools may lead to exterior breakage and elevated routine maintenance costs [32].

To refrain from the unfavorable consequences triggered by conventional methods, many other pavement deicing approaches have been experienced; for instance, hydronic heating fluids [33]–[37], electric heating pipe [38], infrared heat lamps [39], electrically heating wires [40], and electrically heating pavement [2], [19], [47]–[50], [24], [25], [41]–[46]. Over the years, electrically heating pavement system has been adopted in several ways, such as electrically conductive concrete [44], [51]–[53], embedded heating element [19], [41], the sandwich conductive layer [54], [55] scrutinized all of these heating techniques regarding the project's

fundamental scenarios, expenditure, installation and functioning, and efficacy. Nowadays, a couple of the emerging methods for this objective focus on applying the superhydrophobic coating [20]–[22] and an electrically conductive coating [27], [56] on pavement tops. This chapter provides a concise overview of thermal snow melting methods and summarizes the findings from various research works that attempted to melt snow from the pavement in different ways.

2.1 Hydronic Heating Pavement Systems

Hydronic systems circulate warm fluid through a pavement-embedded pipe network to distribute heat to the snowmelt surface. A radiant heating grid, a thermal distribution system, and a heat source make up an HEHPS. Researchers are looking into heat sources that can produce the requisite pavement heat flux at a cheap cost to improve system performance and save operating costs. For small hydronic systems, electric and oil-fired boilers are common heat sources. However, research has been performed for the past 70 years to replace electric and oil-fired boilers as an HEHPS heat source with renewable energy sources. The first geothermal-powered HEHPS was installed in Klamath Falls, Oregon, in 1948 on a critical roadway section. A geothermal well with a downhole heat exchanger provided fluid temperatures of 38 to 54 degrees Celsius. The heated fluid generated a 129.3 W/m2 heat flux on the pavement. This resulted in a snow-free pavement with a minimum air temperature of -23°C and a snowfall rate of 7.6 cm/hr [57]. An experimental program evaluated the performance of an entirely constructed ground-source heat exchanger in an HEHPS study conducted in New Jersey during the 1969–1970 winter season. In the study, Winters (58) discovered that a geothermal HEHPS with an average soil temperature of 13 °C melted a 2.54 cm snow layer in 4 hours. Balbay and Esen [58] used

another HEHPS approach in their study, where they combined a ground-source heat pump installed in-ground boreholes with U-pipe heat exchangers.

2.2 Infrared Heating Pavement Systems

An electromagnetic emission produced in a heat source by the fast vibration and rotation of molecules is referred to as infrared radiation. Infrared systems have been developed and used in various applications, including snow melting, space heating, drying, and other processes. The most common application areas have been pedestrian walkways, emergency access, loading port ramps, and hotel lobby entries. The heat from infrared heaters is delivered instantly, allowing snow to be melted without raising the temperature of the surrounding air space. Snow melting systems using infrared technology are described in depth by the ASHRAE. Overhead infrared heaters are commonly used. This requires a considerable number of infrared heaters spread throughout the snow melting surface. Yuji et al.[18] constructed an infrared snow melting system to melt snow and ice off electronic toll collection lanes, vehicle detectors, and other road equipment. The usage of fossil fuel as a source of heat for the system resulted in significant energy consumption.

2.3 Electric Heating Pavement Systems

Electrically snowmelt systems use hot wires, electric mats, embedded heating elements, conductive coating, or conductive concrete to heat pavement surfaces to ensure that they are free of snow, rather than the hot fluid used in hydronic systems. Electricity is the primary energy source for these systems. The selected heating element should produce the appropriate heating power at the snow melting surface to melt snow efficiently. An energy source (electricity), sensors for assessing weather conditions, heating elements, and system controllers are the major system components. Because of the limited energy source options, many studies have not

concentrated on electric snow melting systems. Rees et al.[35] investigated the performance of an electric pavement snow melting system under transitory situations using experiments and simulations. It was discovered that the needed design heat fluxes with back losses are unaffected by soil conductivity or the presence of insulation. The research also resulted in the creation of computer software for the transient analysis of snow melting systems. Kim et al.[59] investigated techniques to reduce the energy used by electric snow melting equipment on train roads. Power usage was found to be depending on the system's operation time in an experiment. The time it took to operate the system rose as the ambient temperature dropped, while it increased as the wind speed increased, with humidity having no effect. Dyer (5) created an excellent electric heated mat for melting snow and ice to save energy. More research into how to improve electric snow melting systems is still needed.

2.3.1 Embedded heating element pavement systems.

The snow-melting pavement with an electric heating system has shown to be an efficient and controllable technique to overcome the concerns mentioned above. For the embedding heating elements, researchers extensively studied these methods to analyze prospects of snow-melting effectiveness[19], temperature distribution [60], and energy consumption [55]. Lai et al.[19] evaluated the snow-melting ability by providing an adequate embedded depth of carbon fiber grille and embedded spacing of heating wires, as well as using the snow-free area ratio criterion. Yang et al. [61] carried out a deicing experiment to analyze the system's energy consumption, where they devised a design for the heating panel using carbon fiber. Liu et al.[15] found an interrelationship between energy usages, embedded depth, and embedded spacing by two-phase thermal simulation and experimentation. Zhao et al. [60] investigated the temperature distribution on a typical section for various embedded carbon fiber heat wire spacings and

established the maximum allowable embedded depth. Lai et al. [62] studied the construction type, heating power, and temperature field distribution of snow-melting heated pavement in the tunnel portal, as well as the embedded spacing of heat wire. In a nutshell, most researchers developed embedded elements heating systems based on snow-melting efficiency, energy consumption, temperature distribution, and other factors. The temperature differential between the internal high temperature of the electric heating system and the external low temperature of the pavement surface, on the other hand, will considerably enhance the pavement temperature, severe stress, and hasten pavement degradation. So, its necessitates the development of embedding elements heating techniques from the standpoint of mechanical characteristics to supplement the existing research.

2.3.2 Electric conductive concrete pavement.

Among the deicing practices, electrically conductive pavement is probably referred to as the best feasible snow removal method from roads, which is one sort of affordable, proficient, environmentally hospitable, and sustainable approach. To acquire superior Electrically Conductive Concrete (ECC), which must consist of precise quantities of electrically conductive elements. Therefore, the present research study concentrates on generating conductive concrete with conductive filler such as graphite powder, flexible graphite pet sheet, carbon fibers grille, carbon nano-fiber polymer, carbon nickel particles, steel slag, and steel fibers [19], [52], [63], [64].

2.3.2.1 The working principle of electric conductive concrete pavement.

The Electric conductive concrete has two parts to its functioning: transfer heat between layers and deicing. Significant units are following the deicing system: a power supplier, constituents for heat transfer, sensing units for determining climate conditions like snowfall,

outside air temperature level, and humidity, and a process regulation [65]. Electricity is the primary source of these systems [66]. During the snow melting from the pavement surface, it needs to design a proper heating mechanism to supply efficient heating energy to melt snow efficiently. The heat exchange in pavement has three ways: heat transfer by conduction, convection, and radiation. The heat energy is well balanced initially with the pavement-atmosphere interface and occurred heatwave change triggered by thermal radiation, solar energy dissipation, and convection. Temperature differences from the pavement surface and its interior layers arise due to heat flux, and that process leads by conduction. The heat transfer by the conduction process continues through the conductive layer to the top of the pavement. Figure 3 shows the working principle of the electrically conductive concrete pavement.

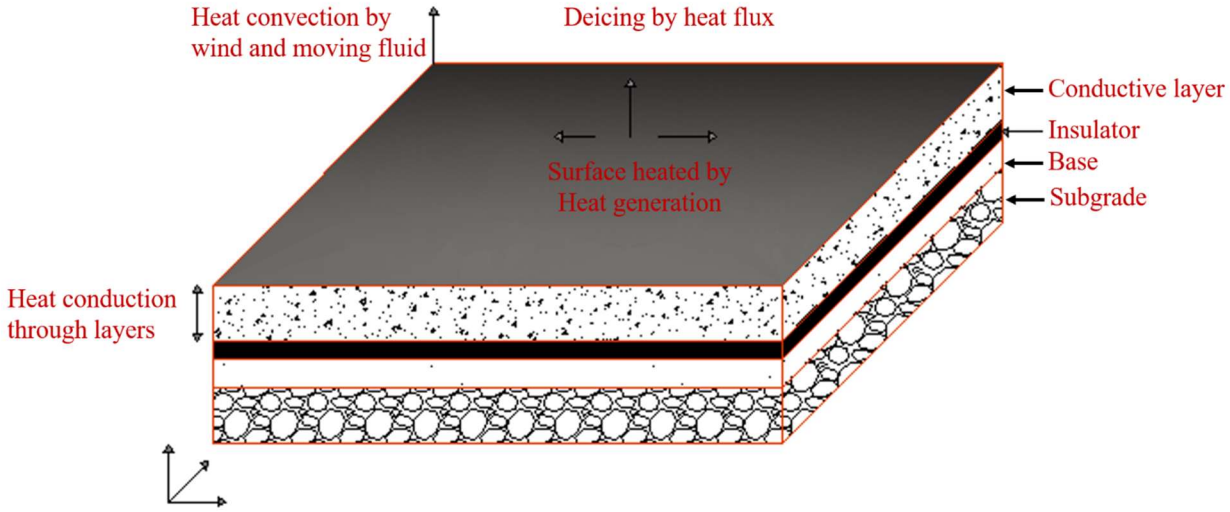

Figure 3: Model of self-deicing electrically conductive concrete pavement.

Conduction: There are two ways the conduction of electricity may occur in the pavement: ionic conduction and electric conduction. Ionic conduction is happened due to the mobility of ions in the pore solution and free electrons; when moved through the fiber, electronic conduction occurred [67], [68]. The conductive concrete is the electrical conductivity, which mirrors the electrical characteristics of its constituents. We need to know the conductivity or resistivity

property of materials to research on attributes of conductive concrete. For that reason, to determine the conductivity of concrete, one must understand the following property: conductivity or resistance, distance, and the area of conductive concrete. According to the first Ohm-law in Equation 1:

$$R=\frac{V}{I} \quad (1)$$

From the second Ohm-law in Equation 2: obtained the electrical resistivity

$$\rho =\frac{RA}{L} \quad (2)$$

The reciprocal of the electrical resistivity is known as the electrical conductivity and is shown in Equation 3:

$$\sigma=\frac{1}{\rho} \quad (3)$$

$$R=\frac{L}{\sigma A} \quad (4)$$

Where I is the measured current, V is the voltage, L is the internal distance, A is the conductive area, R is the resistance, ρ is the electrical resistivity, and Ʊ is the electrical conductivity. Joule's law is the combination of laws regarding heat generation by electricity and the produced power. Besides, this law, known as the Joule effect, is expressed as the heat generation due to the current flow through the conductive materials. Equation 5: where H is the heat generation, the constant current flow is I, R is the resistance of the materials, and t is the duration.

$$H = I^2Rt \quad (5)$$

Convection: is the transfer of heat from one place to another by the moving fluid or wind, and it takes place on the top surface of the ECC pavement. Two types of convection processes occur; one is between the pavement surface and underneath the ice layer, the other between the ice

layers and air above it. This process can be a natural or applied mechanism, which depends on the induced heated fluid motion or air blow. (For the ECC, pavement caused by wind will affect the upper surface of the snow and will be accounted for in the model. Forced convection effects within the snow layer, sometimes called wind pumping, will not be accounted for, nor will the natural convection due to buoyancy through the porous snow layer.)

2.3.2.2 The existing development of electric conductive concrete pavement.

Since the 20th century, efficient and environmentally friendly snow melting solutions have mostly focused on the thermal deicing method. Which technique utilizes heat generation from geothermal, solar energies, hydronic water, and electrothermal to melt snow and ice. Special attention was given to conventional deicing methods since their efficiency, eco-friendly, safety, and feasibility. These days electrically conductive concrete has acquired a prevalent interest in deicing a relatively new building material innovation. That is composited together with dielectric aggregates, water, binder, and conductive materials; and develops heterogeneous material. Table 1 listed previous research studies of ECC pavement, which is a first and foremost utilized by Xie et al.; he applied for a patent (30) right after investigations figured out conductive material as superb conductive stages with high mechanical properties. The performance of conductive concrete for pavement deicing was studied too [69], [70]. Later, Yehia and Tuan et al. explored conductive concrete superimpose on the bridge deck and pavement [71]; steel fibers and steel shaving were utilized for making the conductive concrete. The results have shown that a prototype slab was studied and revealed that electrical conductivity could be gained using conductive elements with required concrete mechanical durability.

Table 1: Summary of research on electric conductive concrete composites.

Research Team	Con. Fillers	Additives (vol.%)	Electrical Resistivity, Ω-cm	Purpose	Ref.
Yehia and Tuan	Steel Fiber	15-20	N/A	Bridge Deck Deicing	[72]
Hou et al.	Carbon Fiber/Steel Fiber	0.58/ 20	N/A	Electrically conductive concrete for deicing	[47]
Tuan et al.	Steel Fiber (SF)	2	5.4×10^{7}	Bridge Deck Deicing	[73]
Gomis et al.	Graphite powder/ Carbon Fiber powder/ Carbon Fiber/ Carbon Nano Fiber	5/5/1-5/0.25-5	1100/1600/730/22	Studied carbonaceous materials to control ice layer in transportation infrastructure	[42]
Derwin et al.	Graphite Powder (GP)	25	N/A	Eliminate the problems of snowy and icy runways	[74]
Sassani, Arabazdeh, and Ceylan	Carbon Fiber	0.75	N/A	applied for ice/snow melting on pavement surface	[3]
Tuan et al.	Steel Shaving (SS)	20-15	2.4×10^{5}-2.2×10^{5}		[73]
C. Tuan	Steel Fiber and Steel Shavings	1.5/20-15	500-1000	Anti-icing	
Wu et al.	Steel Fiber/ Graphite Powder	2/10	45×10^{3}	To investigate the electrical and thermal properties of conductive concrete	[75]
Rao et al.	Steel Fiber/ Graphite	7/15	N/A	To develop special concrete for outdoor snow melting and indoor radiant heating	[76]
Tuan	Steel Fiber and carbon particle	1.5/ 15	300-500	To prevent ice formation on paved surface	[44]

Table 1, cont.

Research Team	Con. Fillers	Additives (vol.%)	Electrical Resistivity, Ω-cm	Purpose	Ref.
Heymsfield et al.	Steel Fiber/Graphite Powder	2.7/17.2	396	To develop ant icing airfield pavement	[45]
Wu et al.	Steel fiber, Carbon fiber, and Graphite	1/0.4/4	322	Developed for pavement deicing	[2]
Sassani et al.	Carbon fiber	0.75-0.98	115-992	Heated airport pavement	[11]
Shishegaran et al.	Steel wire rope and Steel powder	3/5.78	N/A	Route deicing	[77]

2.3.2.3 Preparation of ECC pavement

Conductive materials: The concrete consists of fine aggregate, coarse aggregate, binder, and water, which is recognized as low conductive because of its high resistivity of constituents. For deicing, concrete resistivity values must be less than 1000Ω-cm [73], [78]; fulfilling the requirement should contain conductive materials in concrete than it turns into conventional concrete to the heating element [45], [47], [51], [71], [73]–[75], [78], [79]. The electrical resistivity of concrete rate varies depending on regardless if dried, oven-dried, or air-dried. If it is not dried so regarded as a semiconductor, and its resistivity about 10 kΩ-cm, air-dried concrete resistivity ranges 600-1000 kΩ-cm, oven-dried it is about 108 kΩ-cm [78], and traditional asphalt mix concrete resistivity value 107-1011 kΩ-cm [80]. Those can be modified into conductive concrete by incorporating conductive fillers, and these are considered an essential constituent of ECC pavement. The concrete resistivity decreases along with existing conductive materials since forming conductive networks inside the matrix and achieving the composite's desirable conductivity. Conductive materials have been studied with different shape, type, size, and conductive capability are classified into three categories based on grain dimensions: (a)

powders consisting of aluminum chips, carbon black, graphite [81]–[83], (b) fibers consisting of carbon nano-fiber, carbon fiber, steel fiber, steel wool, graphene, and carbon grill [84]–[90] and (c) solid particles like copper slag, steel slag replacement for the fine and coarse aggregate completely and partly [91]–[94]; stated that electrical resistivity varied from 400 to 2.4×105 Ω-cm, when conductive materials integrated into concrete in percentages from 1% to 20% by volume of concrete [95]. Table 2 presented conductive materials used in the previous studies, where among all of the conductive fillers, carbon fiber (CF) has been shown impressive performance regarding developing ECC successfully because of their higher electric conductivity [95], [96].

Table 2: Summary of conductive materials used for developing electrically conductive concrete.

Conductive filler	**Sand Ratio (%)**	**w/c ratio**	**Resistivity (Ω-cm)**	**Mechanical Strength (Mpa)**	**Ref.**
4%GP+1%SF+0.4%CF	42	0.44	322	40.8	[2]
0.75% CF	n.a	0.56	50	40	[95]
20% SF +0.73% CF	25-33	0.6-0.56	579-38	41-40	[47]
15% GP+1.5% SF	n.a	n.a	200	48	[73]
0.75% CF	51.99	0.26	81-53	30-38	[3]
7% SS, 7% CP, 7% GP	n.a	0.57	833-500	30-17.5	[98]
1% CNT, 2% CNT, 5% CNF,	n.a	0.6, 0.8, 0.85	180, 70, 730	n.a	[42]
17.2% GF+2.7%SF		0.4	396	43	[45]

Beaudoin et al. developed ECC with 100 Ω-cm [68]; during the investigation, they revealed that carbon fiber volume content could reduce 5% to 3% by increasing CF length 1mm to 3mm. Later, Abdulla and Sassani developed 50 Ω-cm ECC mix design by optimizing CF's attribute and aspect ratio using only 0.75% [95], which mix used in the Des Moines International Airport pavement [11]. However, CF water absorption capacity is very high results in compromise on the casting by reducing the workability of the mix [96]. Another concern

regarding CF is costly, so Banthia et al. induced hybrid filler CF and SF, which investigation successfully achieved the lower resistive concrete to minimize the use of CF content [97]. Another mixed filler used by Yehia and Tuan, where they used GP and SF, which applied in the Roca Bridge in Nebraska [44]. Three conductive filler (GP, SF, and CF) combinations were investigated by Wu et al. and achieved concrete resistivity 322Ω-cm [2].

Aggregate gradation: There is no published research study about the suitable gradation of conductive concrete; hence, it is not restricted to an appropriate gradation. The gradation and aggregate size were not explicitly defined, though literature reviews indicated that aggregate gradation for conductive concrete followed the general concrete mix design. In terms of the basic principle of conductive concrete, the mineral aggregate should have adequate voids to fill by conductive materials to enhance the conductivity of the mixer, which is recommended. Simultaneously to ensure the standard mechanical properties of concrete required a superior structural skeleton. Additionally, conductive materials can be an attractive alternative to fine aggregate and mineral filler, which may lead to the pertinent modification of conductive concrete regarding volumetric aspects. Therefore, changing the density of materials should consider and highly suggested that to avoid any danger of conductive concrete mix by declining the mechanical properties.

Mixing procedure: ECC can be prepared following different fabrication methods, which depend on the order of adding conductive materials and divided into three ways: the first admixing method, the synchronous admixing method, and the latter admixing method. 4 illustrates three fabrication methods with the following steps. ECC fabrication requires proper mixing of conductive fillers with cementitious composite, which will influence the even distribution of conductive materials, affecting ECC characteristics such as electrical and mechanical. For

different conductive materials, Table 3 listed appropriate fabrication methods. The joint mixing method is recommended for hybrid materials.

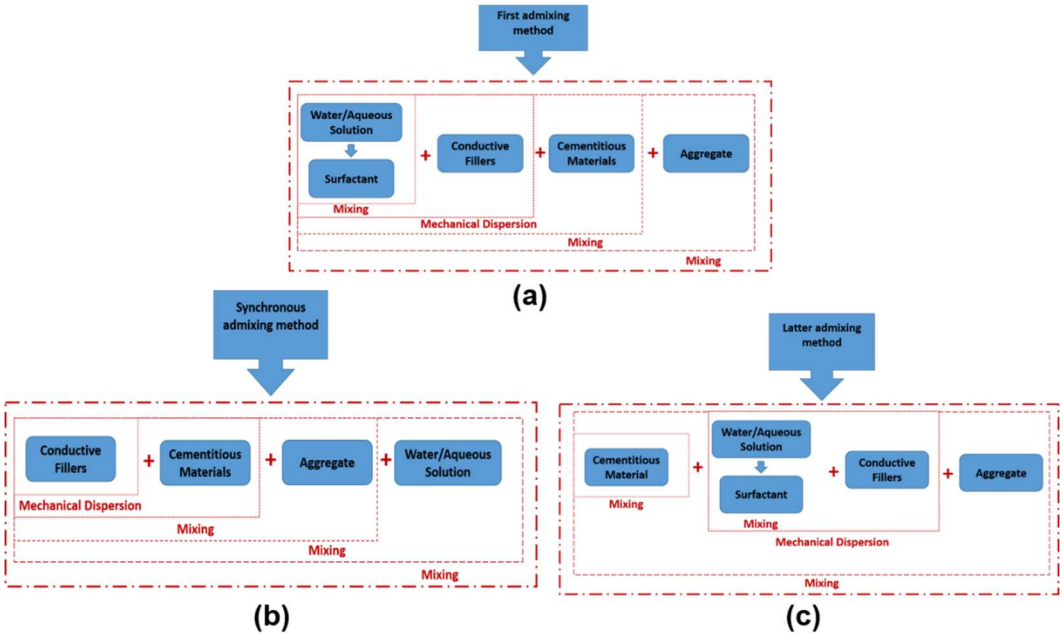

Figure 4: Three mixing technology for fabrication: a) first admixing method b) synchronous method c) latter admixing method.

Table 3: Appropriate fabrication methods for different conductive fillers.

Mixing Method	**Suitable Conductive Fillers**	**Ref.**
First admixing method	CF; CNF; CNT; CB; GNP; NS; NT	[99]–[104]
Synchronous admixing method	CF; Steel shaving; CP; GP; CB	[98], [105]–[107]
Latter admixing Method	SF; GP; CNT; CF	[108], [109]

Dispersion method: Throughout the cementitious matrix blending procedure, it is challenging to disperse conductive ingredients evenly and attain an identical state within the cementitious matrix, which enormous periphery leads to the interplay between particles cause of high van der

Waals force at Nano and macro scales elements. Figure 5 illustrates the optical microscopy images of poorly dispersed carbon fiber and well dispersed in the dispersant solution. The well-dispersed conductive materials form conductive chains even more quickly, whereas the inadequately distributed components remain in fasciculate condition, making it challenging for electron alteration. This can function adequately, prevent forming a cluster, and attain uniform dispersion of conductive materials. Currently, three considerable approaches are practices to enhance the Dispersion: chemical, mechanical, and mineral fillers.

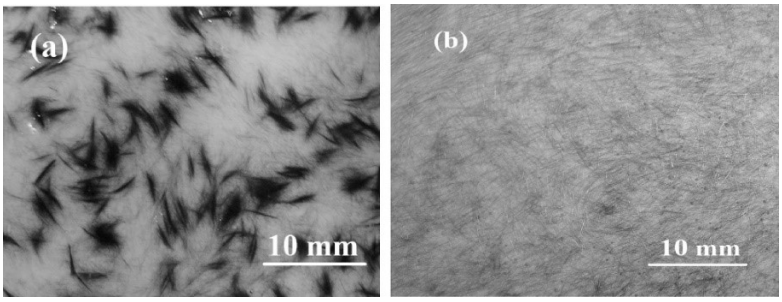

Figure 5: Optical microscopy images of carbon fibers in the dispersant solution: (a) poor dispersion; (b) good dispersion [110].

Mechanical method: There are three methods included in traditional mechanical mixing methods: mechanical stirring, ball milling, and ultra-sonication. The conventional method: Mechanical stirring is not appropriate for the conductive nano-filler due to it is unable to break the bond between particles, and after stopping stirring, it is inclined to re-agglomerate; as a result, uneven distribution of conductive particles. Al-Dahawi et al.[111] investigated different mixing methods and compared them in terms of electrical performance where they involved high-rotational speed mixing and revealed possible best results would get in terms of sheer effect. Although the mechanical characteristics have not been investigated, they cannot firmly say that martial well integrated into the composite. The ball milling method, known as the power milling method, breaks the bond between particles and can retard the nanomaterial

agglomeration. Since it damages the integrity, reduces the aspect ratio of particles, and is harmful to mechanical property, it is not appropriate for the fibrous particle [112]. The well-dispersed nanomaterials can be achieved by adopting an ultra-sonication method, an aqueous solution that uses a surfactant and requires adequate time and energy for good Dispersion. Zou et al. [113] have investigated the ultra-sonication method with the CNT particle and achieved optimal energy with good mechanical properties. To avoid damaging conductive fillers essential to select adequate energy for dispersing materials in the ultra-sonication method. But, to hinder overheating of the suspension, recommended using 20s per cycle for the operation of the sonicator [114].

Chemical method: Chemical dispersion approaches are classified into two categories; one of them is covalent, and the other one is non-covalent. The Oxidant and acid treatments involve chemical adjustments in the covalent process, which modify the materials' surface structure by putting functional groups to the materials' surface [115]. On the other hand, the non-covalent method is based on non-covalent interaction, for instance, particles' physical absorption. That keeps the structure intact from the material's addition and induces no harm to the material properties[116]. Endorsed surfactants that is one of the non-covalent methods for material dispersion. The covalent and non-covalent method influence was investigated by Kwon and Yu [115] while analyzing the piezoresistivity characteristics of the CNT cement matrix. Compared to the non-covalent method, the matrix fabrication with the covalent process shows poor performance since suspended surfactants create blocks between the CNT particles [115]. Nevertheless, chemical customization may harm the materials' structure and deteriorate the mechanical and other properties [117]. Thus, for materials dispersion, the non-covalent method along the ultra-sonication approach was adopted in many research studies. Compared with

micro-sized particles, the nanomaterial property with high-aspect-ratio, the broad area of surface difficult to make Dispersion with chemical, thus recommends using the ultrasonic treatment. Nevertheless, to hinder forming re-agglomeration of particles, before ultra-sonication, add adequate surfactants with an aqueous nanoparticle solution and apply the combination of chemical and mechanical for dispersion.

2.4 Electrically Conductive Coating

In order to make a desirable electrically conductive composite, which should have a sufficient amount of conductive materials along with binders; as conductive materials, various carbonaceous materials have been used in previous researches, such as carbon nanofibers [86], [88], graphene [90], or carbon black [81]. The conductive fillers require to disperse evenly while blending with binders, which creates enough conductive paths inside the composite. Thus, it needed a suitable binder to make this synthesis and the ability good adhesion to substrates. As a binder, numerous types of polymer can be used in the composite; for instance, epoxy resin has been used as a binder and applied on various substrate such as portland cement concrete (PCC) surface [118] and asphalt concrete pavement surface [21], [119]. The polyvinylidene fluoride (PVDF) has been used as a binder to create the superhydrophobic coating on the substrate [88], [120], [121], whereas it appeared low strength and weak bondability. In recent years, polyurethane (PU) polymer has increasingly gained attention as a coating material; since it has a superior binding ability with the substrate. Waterborne polyurethane (WPU) has become popular than solvent-based polyurethanes because of its minimum toxicity that positively affects surface coating applications. Moreover, WPU has elegant properties such as flexibility, abrasion resistance, versatility, and far-reaching substrate applicability [122]–[124]. The WPU has been used as adhesives and coatings on different substrates, for instance, plastics, leather, textiles,

paper, rubber, and wood [125], [126]. Different conductive fillers, including glass fiber, carbon nanotube, carbon fiber, carbon black, and graphite so forth, were used right into polyurethane material alone or combined to enhance the thermal stability, mechanical toughness, and electrical conductivity of polyurethane-based compounds. Compared to other fillers, graphite (GP) is assumed to be less costly and had an outstanding performance regarding both conductivity and toughness. Graphite powder (GP) with micrometer-sized particles might boost network microstructures channels, which helps to flow current through the composite properly. The composite with WPU and different dosages of GP exhibited excellent electrical property as well as thermal stability.

2.4.1 Conductivity mechanism.

Conductive elements are induced into the polymer matrix to improve the conductivity of the composite coating, followed by the theory of conductive pathways. The conductive paths can be formed inside the composite after endorsing a suitable amount of conductive materials since they are connected, enabling flow current through it, enhancing conductive attribution of composites [99]. However, it increased the cost of the conductive coating compared to the traditional coating. Mitigating such concern, it is essential to uncover the appropriate conductivity enhancement mechanism and choose the methods that offer lower-cost but provide excellent conductivity, including good mechanical properties. The small dosage of conductive filler is endorsed into the polymer matrix that transforms the insulator into a conductive material and exhibits conductive characteristics if enough conductive paths can be formed. Therefore, it needs to determine the optimum limit of conductive fillers that follow statistical percolation theory. That is defined as a limit that has occurred suddenly in the mixture after going beyond the quantitative limit attributes more remarkable performance, representing the relationship

between conductivity and amount of conductive filler [127]. Beyond the percolation threshold, no conductive paths formed into the composite; however, it radically changed after adding conductive particles and started to create conductive paths and reach the percolation threshold. Figure 6 shows that ECC has some zones, including insulated, transition, conductive, and saturated (fiber overlapped) zones. In the percolation threshold zone, conductive particles start contacting each other and making bridges that decrease composite resistivity with several orders or even more [128]. However, the insulated zone shows tiny changes of resistivity reduction, even the same as the conventional composite, and the saturated area also offers the same characteristics. For the insulated zone, no effective conductive paths were formed because the conductive fillers could not bridge each other. On the contrary, conductive fillers are completely saturated for creating conductive paths in the filler overlap zone, so additional conductive fillers may not form more conductive paths, which shows a slight resistivity reduction.

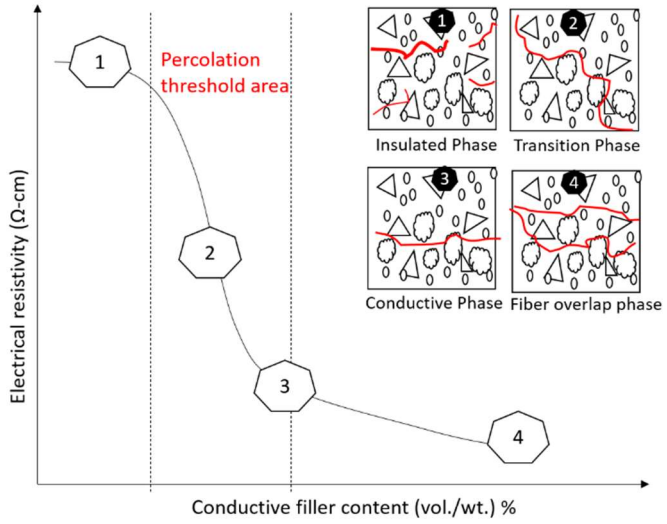

Figure 6: The different zone of the electrically conductive composite.

Considering the percolation theory increases the conductive filler reduces the composite resistance. However, it will increase the poor workability of the coating due to the higher water absorption ratio of fillers that leads to agglomeration of fillers, so the conductive filler

concentration is a crucial factor. The literature shows that the aspect ratio of conductive filler greatly affected the conductivity of the composite; for instance, a smaller diameter of conductive fiber can better decrease the resistivity than a larger diameter of fiber [108]. It is also observed that the small diameter of fiber/particle has a good efficiency in dispersing because of lower surface energy. In contrast, the larger particle has not, therefore small-diameter particles disperse quickly than larger particles [129]. Nevertheless, the larger diameter particle can show a more remarkable distribution ability than nanoparticles [130]. The length of conductive fiber affects increasing the conductivity; using the same filler concentration with a longer length of fibers provides lower matrix resistivity [101]. Al-Dahawi et al. [131] have proved that longer fibers trigger lower resistivity outcomes because longer fiber lengths can offer more constant conductive paths by overlapping with lower concentrations [127]. The conductive path formation has also depended on filler dispersion, which size and types can play a vital role along with filler content and w/c ratio. In general, the dispersion effect can be improved by using a specific limit of surfactant that helps minimize water-reducing impact. However, excessive use of surfactant can create a bubble inside the composite, thus ruining the conductive path formation due to form spacing between conductive filler. To good dispersion of conductive fillers beneficial to use a high curing agent ratio that helps increase the workability of coating; however poor workability influences the formation of the conductive path. So, it is crucial to adjust the polymer/curing agent ratio to ensure good workability.

CHAPTER III

METHODOLOGY

3.1 Materials Selections

The study's concept came from the usages of thermoplastic marking, which is already commonly employed on pavement surfaces. Thermoplastic is the best feasible striping material because it is long-lasting, efficient, and does not alter the pavement's structural properties. So, the strategy was to change thermoplastic characteristics to make it more electrically conductive; however, the cost is a significant restriction. Later, it was discovered that the thermoplastic is higher resistive than its adhesive component resin. So, it must be blended with a well-conductive material that is inexpensive, durable, and has good dispersion properties.

3.1.1 Conductive materials.

In the preparation of electrically conductive coating composite, required to consider both the electrical resistivity and thermal conductivity of conductive phase material. Carbonaceous materials possessed the lowest resistivity and superior thermal conductivity among commonly used conductive materials shown in Table 4. Compared to other fillers, Graphite powder was assumed to be less costly and had an outstanding performance regarding both conductivity and toughness. Graphite powder with a carbon content above 90% and micrometer-sized particles might boost network microstructures channels, which helps to flow current through the composite properly.

Table 4: Electrical and thermal characteristics of different conductive fillers.

Metal	Silver	Copper	Aluminum	Graphite	Carbon nanotube
Electrical resistivity ($10^{-6}\Omega$-cm)	1.55	1.7	2.7	-	-
Thermal conductivity (W/m-K)	419	385	210	2000	3000-3500

The GP has the including properties: high-temperature resistance, friction resistance, corrosion resistance, good chemical resistance, heat conduction, and electrical conductivity. Hence, micrometer-sized GP has been used in this study shown in Figure 7 and its properties are listed in Table 5.

Table 5: Properties of micrometer sized graphite powder.

Properties	Diameter/μm	Specific Gravity	Carbon content /%	Electrical conductivity/(S/cm)	Ash/%	Moisture/%
Value	44	2.26	99.35	28.25	0.65	0.2

3.1.2 Adhesive materials.

The composite coating is supposed to be used on the PCC pavement surface, hence intended for reducing curing time, which will enable shortening the closing time for traffic on the coated surface. Therefore, instead of incorporating any solvents, this study used fast-drying water-based polyurethane (WPU), and epoxy resin was selected as bonding materials shown in Figure 7.

The primary performance of WPU and Epoxy are shown in Table 6. These are needs uniform stirring bonding materials and curing agents in a 3:1 ratio, and they were added with conductive phase materials to get desirable the conductive composite.

Table 6: The basic properties of waterborne polyurethane and epoxy resin.

Materials	Solid content / (%)	VOC content/ (g/L)	Viscosity mPa-s (20°C)	Ph	Proportion	Curing (Set to touch)/hr
Waterborne polyurethane (WPU)	57	72	-	6-7	1.12-1.15	6-7
Epoxy Resin	48-52	63	400–1000 mPa·s	2-7	1.02-1.09	9-12

Figure 7: Used materials to produce electrically conductive coating composite.

3.1.3 Electrodes.

Conductive coating applied on the top surface of specimens to work as a heating element. Doing so needs lower surface resistance of applying the coating, which can be determined by a digital resistance measurement device (Keithley 2400). A two-sided electrode has been used to

measure the resistance of WPU-GP/EP-GP, and Figure 8 depicts a diagram of the specific resistance measurement. Since higher conductivity properties, electrodes have a key role in EHPS supplying electricity through the conductive coating. The copper tape was placed inside the two ends of the coating as an electrode, which improved the electrical connection since a low dosage of GP could not be exposed to the surface.

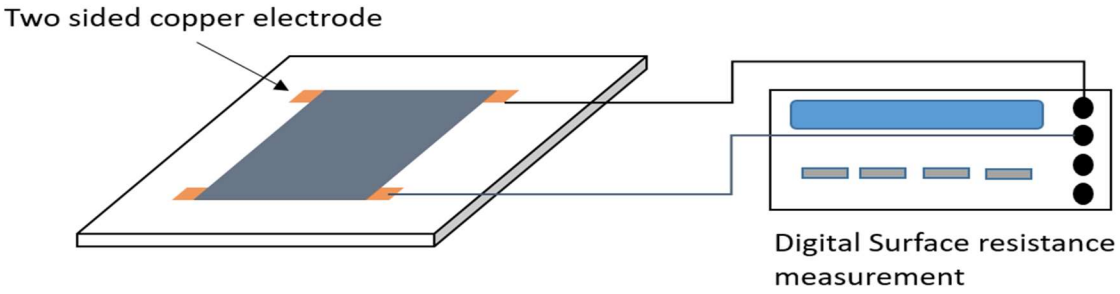

Figure 8: Two-electrode electrical surface resistance measurement.

3.2 Properties of Conductive Materials

In order to validate the efficacy of the materials used in this study, two parameters were measured: surface resistivity and heating ability of the prepared materials. The techniques of inquiry for these features were briefly mentioned in this section.

3.2.1 Surface resistivity measurement.

To achieve the desired electrical conductivity of the mixture, required to determine the optimal dose of conductive filler with the polymer content, using a method called percolation threshold, which is an excellent method to explain the electrical behavior of composite [132]. The polymer content acts as an insulator in the mixture, so the volume fraction of conductive filler should be greater or equal to the percolation threshold [88], [133], [134] to achieve its higher electrical conductivity. Therefore, an acceptable amount of conductive filler needs to add with polymer contents, which help to form the continuous conductive paths in the whole matrix or edge to edge. The range of conductive fillers usage in the mixture at which electrical

resistivity decreased rapidly, which is known as the percolation transition zone [135]. By increasing the volume fraction of conductive fillers within the percolation transition zone, the electrical resistivity of the composite reduces several orders of magnitude. It reduces while adding more conductive filler above the percolation threshold zone; however, resistivity decreases at a lower rate since the network formation by conductive elements is already saturated in the composite [132]. As the conductive filler dosage continues to increase in the mixture, its viscosity increases, making it challenging to apply to the sample surface [132]. Therefore, it is required to determine the percolation transition zone of WPU-GP and GP-EP composite by containing different volume fractions of GP in the mixture and shown in Table 7. Two coated substrate samples, such as wood and PCC, were prepared using the mixture proportion given in the table to measure surface resistivity shown in Figure 9.

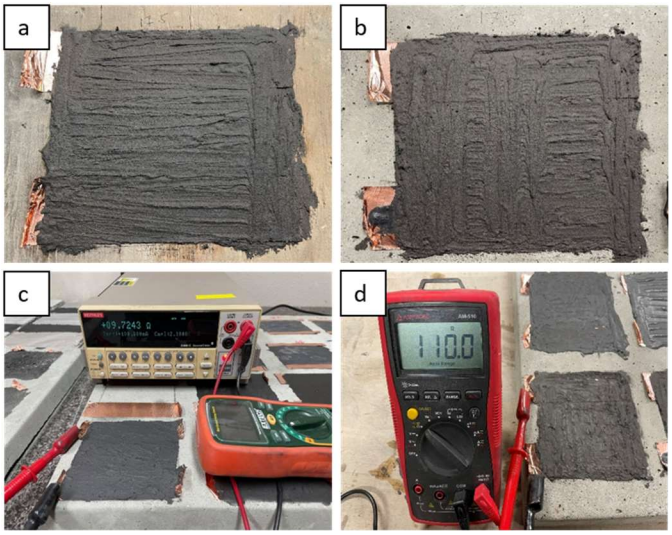

Figure 9: Coating applied on the (a) wood substance (b) concrete substrate (c) two probe resistance measurements of coating using (c) Keithley 2400 (d) digital multimeter.

The wood substrate has been used to measure the electrical resistivity of the surface since the dry wood has low conductivity, so there was no interference with the resistivity measurement [27]. The coating specimens were prepared on the air-dried PCC surface to simulate the intended

real idea during application on the concrete pavements. The final results were prepared by taking on an average of using both specimens, and each type has three replicates. The two-sided conductive copper tape was applied to the ends of coating specimens to measure the resistance. Since low dosages of GP, especially in the composite, have a chance not to expose properly and may not contact the electrode. For this purpose, copper tape has been attached inside the coating and helps voltage applied during resistance measurement. This study used two probe methods [46], [136] to determine the electrical resistivity, which is more accurate and reliable for measuring the surface resistivity of the coating. A digital DC source multimeter (Keithley 2400) was used to measure resistance value with 1 s to avoid polarization [137]. The ratio of applied voltage on the attached two-sided electrodes in the coated surface during current flow through one electrode to another know as the surface resistance. Figure 10 depicts the pair of copper tape used in the specimens' coated surface and testing voltage applied through these electrodes. The surface resistance value depends on the used conductive materials and electrodes configuration [138].

Table 7: The proportion of materials for WPU-GP/EP-GP conductive coating to determine the percolation transition zone.

GP (% Vol.)	WPU/EP Content (gm)	CA Contents (gm)	GP Content (gm)
0.00	15.00	5.00	0.00
2.50	14.63	4.88	1.13
5.00	14.25	4.75	2.26
7.50	13.88	4.63	3.39
10.00	13.50	4.50	4.52
12.50	13.13	4.38	5.65
15.00	12.75	4.25	6.78

17.50	12.38	4.13	7.91
20.00	12.00	4.00	9.04
22.50	11.63	3.88	10.17
25.00	11.25	3.75	11.30
27.50	10.88	3.63	12.43
30.00	10.50	3.50	13.56

All measurements were conducted at room temperature and relative humidity in the air. Each coating was controlled with the same thickness ensuring at a different point, and width and length measurements of each specimen counted with 0.01mm precision. The parallel strip method is used to determine the surface resistivity per square (Ω/sq.) [139], and the dimensions are used to do this. It was calculated according to Eq. (6): where surface resistivity is denoted as $\boldsymbol{\rho}_s$, which is defined as the ratio between testing voltage per unit length to the supplied surface current to the width of coating specimen [138]. To determine the percolation transition zone, surface resistivity was plotted against the GP contents (% Vol.) in the coating.

$$\boldsymbol{\rho}_S = R_S \frac{D}{L} \qquad (6)$$

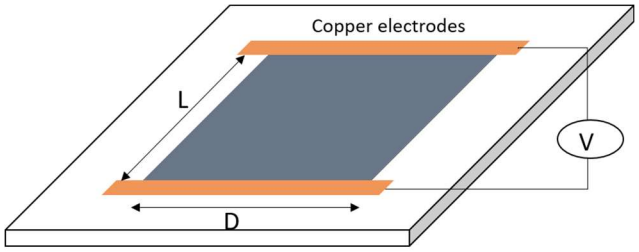

Figure 10: Using parallel strip method for determining surface resistance/resistivity.

3.2.2 Surface heating measurement.

The surface heating test was performed on the wood and PCC substrate specimens to relate the surface resistivity percolation results. To do so, specimens' surface temperature rising

was measured using an infrared thermometer during AC voltage supplied by the time. The wood-substrate samples were investigated when applied voltage was 30V and constant frequency of 60Hz for 5mins to determine the range of GP contents. Since this construction method intends to use on the airfield pavement, therefore, to evaluate the performance of composite coating on the PCC substrate, the resistive heating capability of coating on the concrete substrate was investigated with selective dosages. The GP dosage rate was used 2.5, 5, 7.5, 10, 12.5, 15, 17.5, 20, 22.5, 25, and 27.5% volume of the total composite volume, which are selected according to the percolation threshold zone determination test, and specimens were prepared with three replicates. At different rated voltages (10V, 20V, and 30V) with constant 60 Hz, AC power supplied through the copper tape and measured temperature rising with an active infrared thermometer is shows in Figure 11(b). The measured surface temperature was recorded as explained above for each specimen with a 10 to 30 V AC power supply for 30 minutes. Since the ambient temperature of the actual field is below freezing temperature, simulating samples were kept in the fridge for 12 hours. Specimens achieved -17°C and performed the surface heating test presented in Figure 11(c) and (d). The 60 Hz power supply with 10, 20, 30, and 40V respectively was applied to specimens for 30 minutes, and using an infrared thermometer recorded results presented in Figure 11(e).

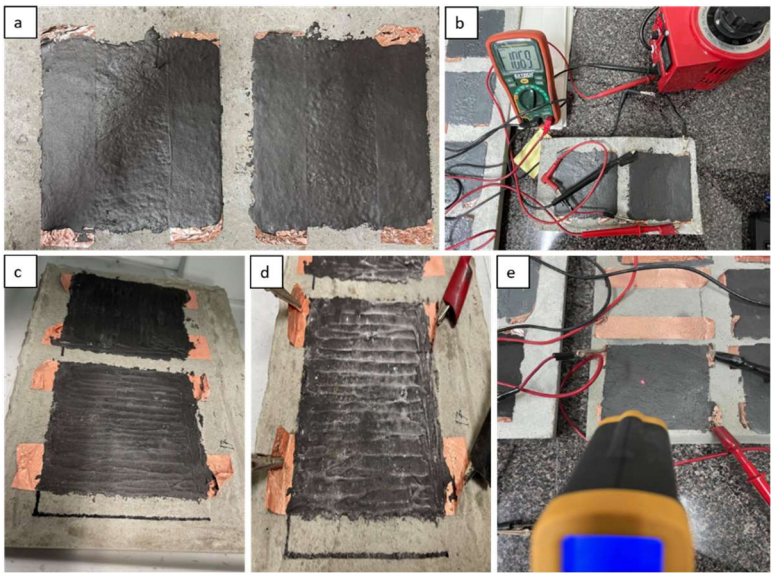

Figure 11: (a) Prepared composite coated on the concrete mat (b) required power supply for measuring surface heating test at room temperature (c) specimens kept in the fridge for 12hrs (d) frozen specimen ready for surface heating test (e) recorded increasing surface temperature by active infrared thermometer.

3.3 Experimental Setup

The experimental setup has been divided into two sections, which are described in this section: the preparation of the materials and the construction of the pavement specimens using the materials that have been prepared.

3.3.1 Preparation of electrically conductive coating.

To begin, oven-dried GP and WPU/EP were stirred in the pot for 3 minutes at 250 rpm, followed by 1 minute of high-speed stirring at 250 rpm to ensure uniform mixing. The hardener was then added to the mixture, and the liquid mixture was stirred at a high speed for 250 rpm for 4 minutes. In order to maintain the proper coating dimension on the specimen surface, cuboid plastic molds were used to form the specimen. The coating had two copper tapes (20 mm x 50 mm) embedded in it for connecting to a current source through the composite surface. Finally,

the prepared mixture was slowly poured into the mold, and Figure 12 depicts the composite fabrication process.

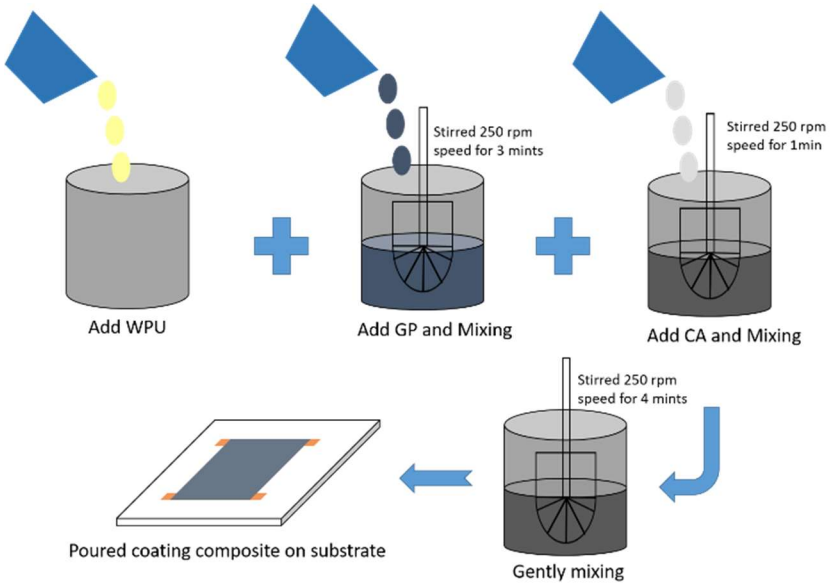

Figure 12: The fabrication procedures of WPU-GP/ EP-GP.

3.3.2 Pavement construction.

A more sustainable construction method of electrically conductive concrete included procedures for determining the contents of the material of the coating composite to create a well conductive coating, the distance between using parallel coating strips, and the heating performance of exposed and sandwich specimens, among other things. The surface resistivity and heating test results of coating were used to determine the properties of composite. Based on heating efficiency during power supply, the coating thickness and spacing were investigated. Two types of specimens were prepared to investigate the heating adequacy: an exposed coated surface and a coated surface covered with another concrete layer (30mm), referred to as a sandwich. This is done to protect the coating layer from water runoff, chemicals, tire abrasion, smooth surface, etc. Finally, by supplying specific voltage applications, the surface heating efficacy of both types of prepared specimens was investigated at room temperature and below

freezing temperature. The graphical procedures for designing a more sustainable construction method for heating pavement surface are depicted in Figure 13.

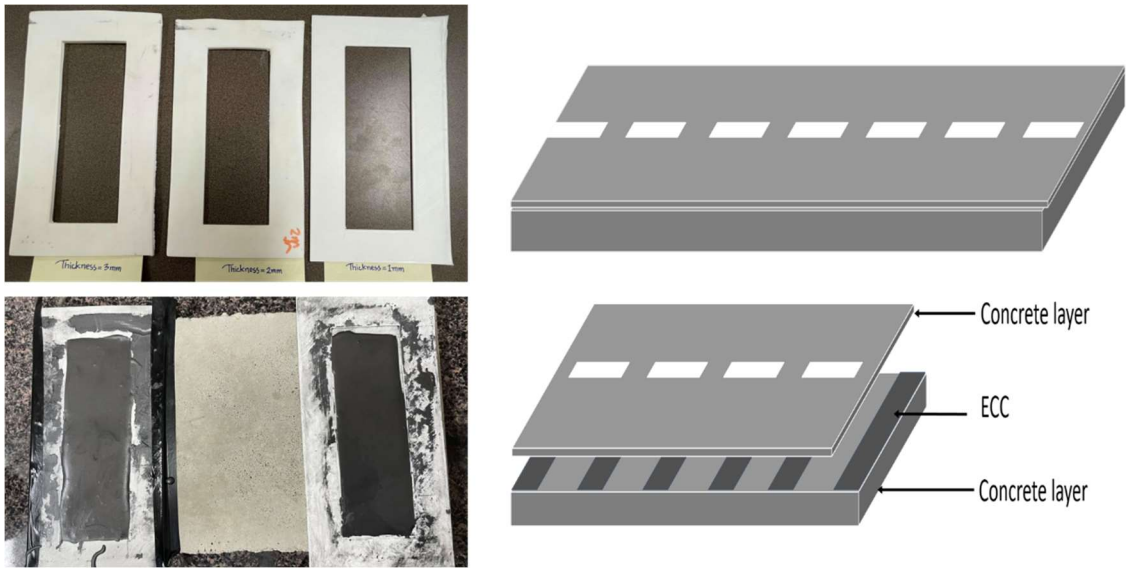

Figure 13: The graphical representation of a new construction method of electrically conductive concrete.

3.4 System Components

The EHPS system comprised some key components, including electrically conductive coating (heat generation element), copper tapes, Keithley 2400, a temperature-measuring instrument (infrared thermometer), a multimeter, electrical wiring, AC voltage variables power source, and a freezer shown in

Figure 14. The experimental design was controlled by infrared thermometers and a digital multimeter, providing real-time specimen surface temperature and required freezing temperature during specimen tests conducted below negative temperature(-17°C/1.4°F). Furthermore, it helps to prevent overheating, which allows for lower energy consumption when the pavement surface temperature rises sufficiently. A digital multimeter controls the power source, allowing for analysis of the EHPS's heating performance across various power supply ranges. The proposed

construction method would be either applied as a surface layer of newly constructed pavements or as an overlay layer on the top surface of the existing pavement after recommended surface preparation, which can be helpful to decrease construction costs by eliminating new construction. The proposed method is no longer necessary to construct thick electrically conductive concrete layers that heat the pavement surface and melt snow where it accumulates. As a result, there are benefits such as cost contrast, maintaining pavement mechanical strength, chemical resistance, weather resistance, UV resistance, and a simple operational setup.

Figure 14: System components used in this study.

3.5 Experimentation

The experiment was divided into two tasks: first, determining the surface resistivity and heating capacity distribution of the materials, and second, determining the efficiency of the construction method. After that, the final experiments concentrated on determining the impact of its parameters, such as strip thickness and spacing on pavements, as well as the voltage supplied and the percentage of GP.

3.5.1 Initial experiments.

For measuring the resistance of the coated surface, two types of substrates are used: wood and PCC. The dry wood substrate was used to test the coated surface's electrical resistance because it is low conductivity and did not interfere with the resistance measurement [27]. The coating specimens were prepared on the air-dried PCC surface to simulate the intended real idea when applied to the concrete pavements, which was the project's goal. The two-sided conductive copper tape was applied to the ends of coating specimens to measure the resistance. Because low dosages of GP, particularly in the composite, have a chance of not exposing properly and thus may not contact with the electrode. Copper tape has been placed inside the coating for this purpose, and it aids in the application of voltage during resistance measurements. The coated substrate samples, such as wood and PCC, were prepared to measure surface resistance

The GP dosage rate was 2.5, 5, 7.5, 10, 12.5, 15, 17.5, 20, 22.5, 25, and 27.5 % volume of the total composite volume, which were selected based on the results of the percolation threshold zone determination test, and each specimen were prepared in three replicates. Fig. 16(e) shows AC power supplied through the copper tape at different rated voltages (10, 20, and 30V) with a constant 60 Hz and measured temperature rising with an active infrared thermometer. The measured surface temperature was recorded for 30 minutes for each specimen with a 10 to 30 V AC power supply, as described above. In order to simulate field conditions where the ambient temperature is below freezing, simulating samples were kept in the refrigerator for 12 hours. The specimens reached a temperature of -17°C, after which they were subjected to the surface heating test .

3.5.2 Construction method functional test.

To test the functionality of the proposed construction method under various ambient temperature conditions, laboratory-scale specimens were built. The test specimen was 300mm x 150mm x 30mm in size, and specimens were coated with electrically conductive composite to substantiate the construction method. The coating was applied as a single strip on the concrete mat, and the distance capable of heating was measured. It was used to set the coating spacing for the final experimental setup's testing specimens. Thus, the prepared composite was applied to the surface of the specimen, which had a coating strip size of 150mm x 50mm and was referred to as the exposed specimen after it had been dried. Comparing its performance to another type of specimen, such as a sandwich, which was prepared by covering an exposed coated surface with a 30mm thick concrete layer. When the supplied voltage was 50V for 90 minutes, two specimens were investigated to determine the heat conduction effect of a single strip when the temperature was approximately 23.6°C. External heat can interrupt the heating test, and generated heat can flow outside of testing specimens, so all sides of concrete mats were insulated except the top surface specimen.

Figure 15 depicts the prepared specimen heating behavior at different distances from the applied coating during room temperature conditions before and after the power supply. After the test section had been sufficiently energized, the surface temperature began to rise at various distances. The surface temperature differences between the control mat and the coated concrete mats demonstrate the heating effect of the construction method. The temperature distribution within the mats' surface is shown in

Figure 15, and the heating effect from the coating was significant up to 12.5cm c/c. It was found that heating both exposed and sandwich specimens at room temperature worked well and

that the distance between strips could be used to construct testing specimens for the final experiment setup.

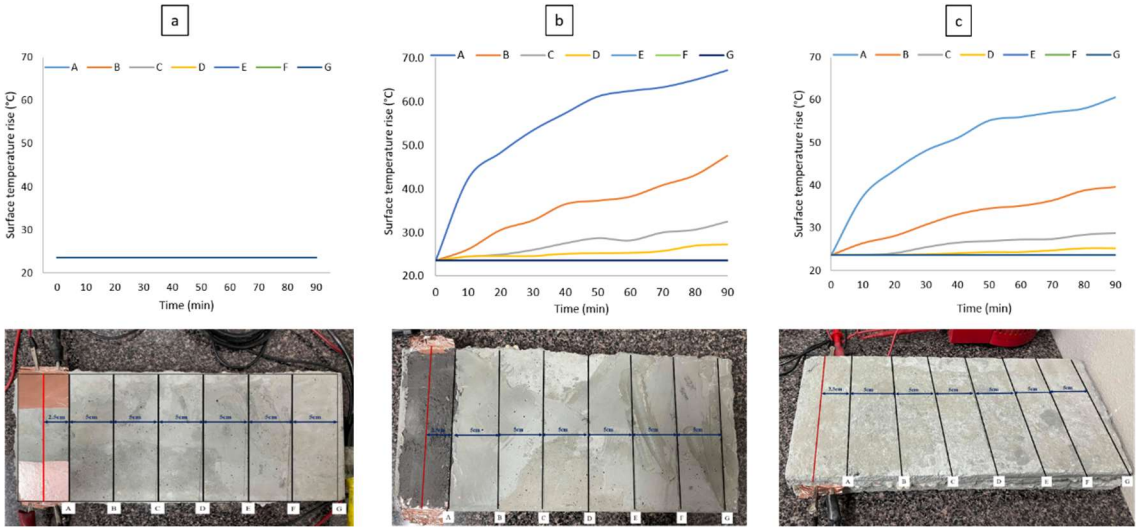

Figure 15: The applicable coating distance determination for parallel coating stripping (a) control section, (b) exposed specimen, (c) sandwich specimen.

Further studies used 15cm and 20cm c/c parallel strip distances for coating application to validate the construction method. During the investigation, three coating thicknesses, 1, 2, and 3mm, were cast in coating configuration. Based on the heating capability of composite produced by WPU, the conductive coating of the GP contents was calculated to be 17.5, 20, 22.5, and 25% of the total. The GP fractions that were considered for EP-based coating were 12.5, 15, 17.5, 20, and 22.5 percent, according to the initial experiments. When coating was employed as a WPU-GP composite, the testing mat received alternating current energy at voltages of 40, 50, and 60V from a voltage variable power source. The high voltage supply of the EP-based coating, on the other hand, began to burn, therefore for this composite voltages, 30, 40, and 50V were used.

Figure 16(a) and (b) depict the applied coating configuration for the final experimental test, as well as the setup for the surface heating of the specimens that have been prepared. When

specimens are exposed to below freezing temperatures, the required time for reaching 0°C of preconditioned specimens (-17°C) is also evaluated and shown in Figure 16(c) and 18(d).

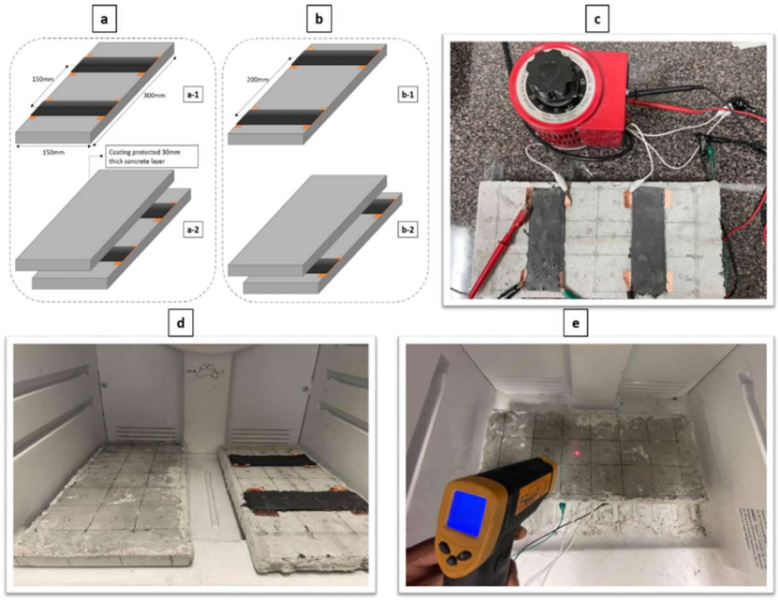

Figure 16: Coating configuration at (a)15cm c/c, (b) 20cm c/c, (c) surface temperature rising measured at room temperature, (d) concrete mats kept in the fridge for 24hrs, (e) recorded surface temperature at -17°.

CHAPTER IV

RESULT AND DISCUSSION

This part discussed the preliminary performance findings of coating composite (WPU-GP, and EP-GP), the surface heating performance of prepared specimens, and the parameters that influence the proposed construction methods regarding rising surface temperature.

4.1 Surface Resistivity

Specimens' surface resistivity was investigated, and the results obtained from each replicate were averaged for each specimen. Figure 19. shows the trends of changing surface resistivity of WPU-GP, and EP-GP specimens at different fraction volumes of GP. Three regions can be observed in the curves of Figure 17 the insulator, semi-conductive, and conductive. In terms of surface resistivity, the percolative behavior is known as the abrupt change in surface resistivity with the incorporation of conductive elements. For instance, GP at a specific dosage rate, the WPU-GP, and EP-GP composite turns insulator to conductive composite presented in Figure 17. The insulating feature has been illustrated for WPU-GP when incorporated up to 7.5 % volume fraction of GP and rapidly reduced a few orders of magnitude at 10% of GP content. At this stage, conductive paths start to form from edge to edge of the whole composite and show the insulator's characteristics to conductive composite. The surface resistivity was continued to decrease while increasing the content of GP; when it contained 20% of GP, the composite was changed semi-conductive into conductive. However, the magnitude of reduction was marginally

above 20% of GP content. At this stage, the GP volume content reached the percolation threshold value and formed continuous conductive paths, which enabled current flow through the WPU-GP composite.

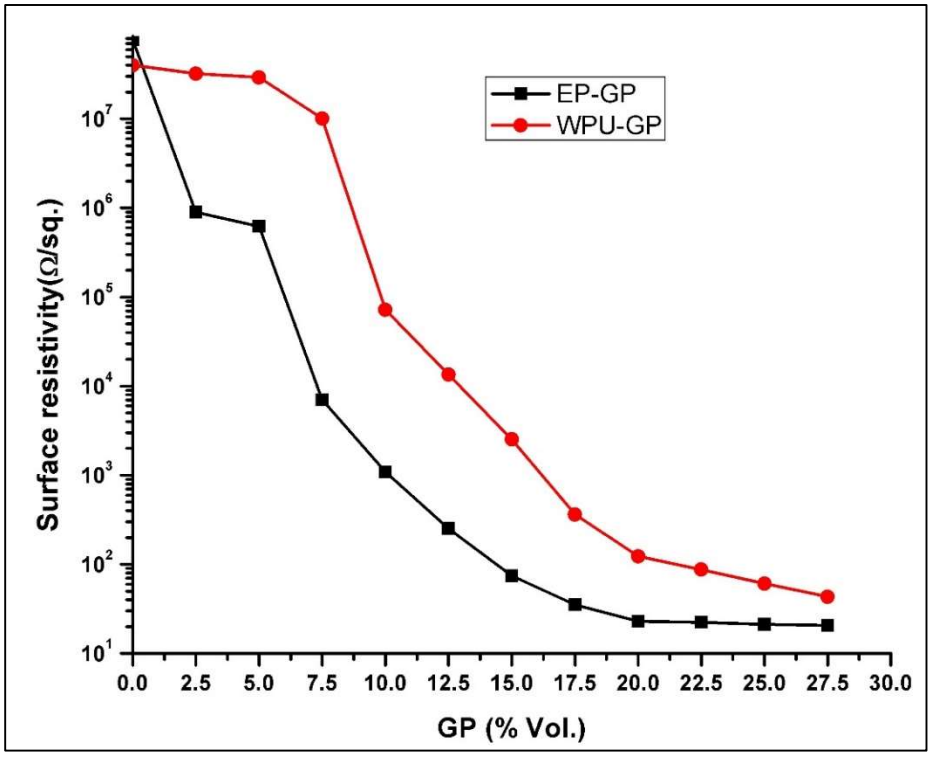

Figure 17: Surface resistivity vs GP (% Vol.) content of WPU-GP and EP-GP composite.

In contrast, the EP-GP composite transitions from being an insulator to becoming a semiconductive material when GP concentration is increased to 7.5%. Composites with increased Gp percentage volume had lower surface resistivity, which decreased in direct proportion to the increase in volume. A 12.5 percent GP concentration produced conductivity characteristics in the composite, whereas an increase in the concentration to more than 20 percent resulted in a decrease in surface resistivity that was barely noticeable and shown in Figure 17.

4.2 Surface Heating Capacity and Distribution

The surface heating capacity of WPU-GP specimens was measured and recorded within 30 min at room temperature. At first, surface heating capacity was investigated with coated (wood) specimens while power supplying at 30V to select the GP dosage rate. Wood specimens were shown no heating effect up to 12.5% GP contains, and has changed abruptly along as increasing the GP contains. Figure 18 presents the average records were reported corresponding to the duration for each WPU-GP coated PCC specimen.

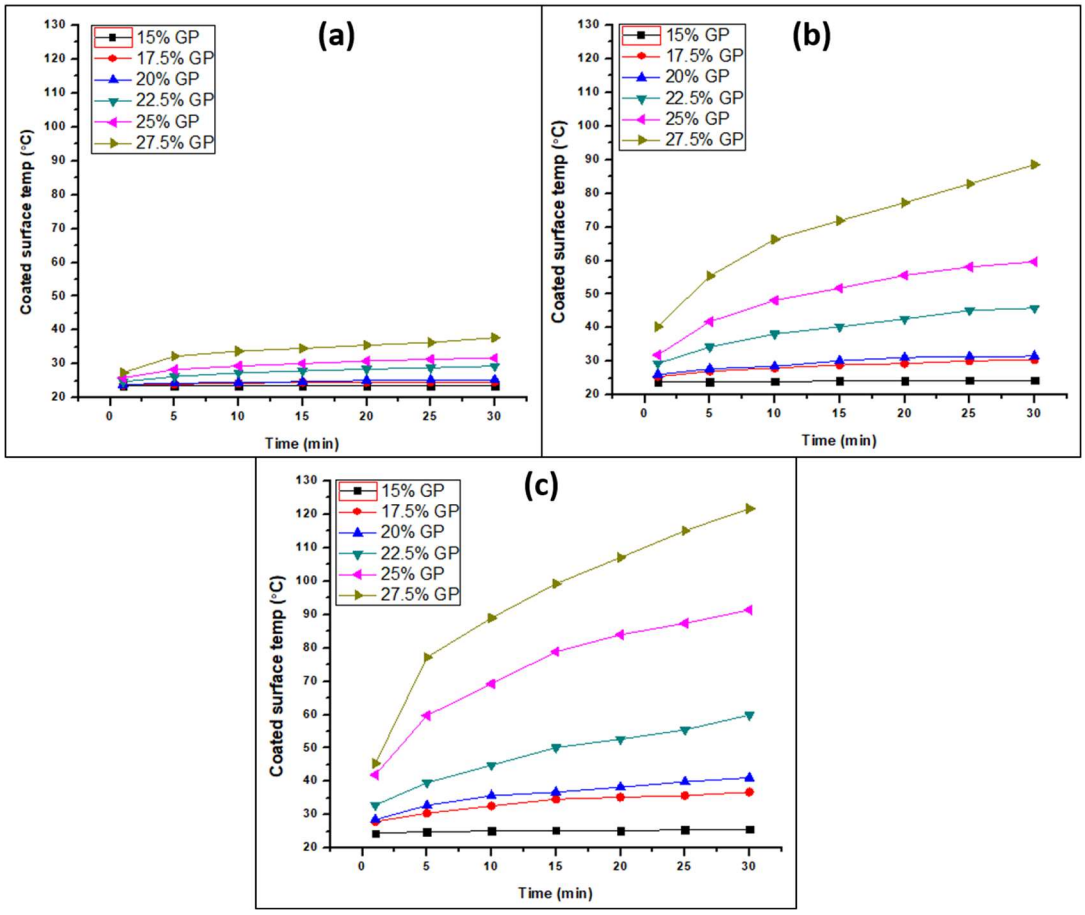

Figure 18: WPU-GP coated surface temperature increase vs time with different content of GP (Vol.%) at supply power (a) 10V (b) 20V (c) 30V.

The result shows a trend of elevating the average surface temperature along as increasing with GP content in the composite and voltage. Up to 17.5%, GP contains coated surface has shown a minimal change of surface heating at 10V, 20V, and 30V. Figure 18 shows the surface temperature rising performance of each WPU-GP with GP volume content of 15%, 17.5%, 20%, 22.5%, 25%, and 27.5%. For GP contents of 20%, the average surface temperature was increased by 2.16°C, 7.3°C, 17.9°C, respectively, at 10V, 20V, 30V within 30 min. In comparison, the surface heating was significantly observed when GP content was above 22.5% of GP. However, the experiment record has been noticed extreme spot heating at some point and left some unheated spots when GP contents above 22.5%.

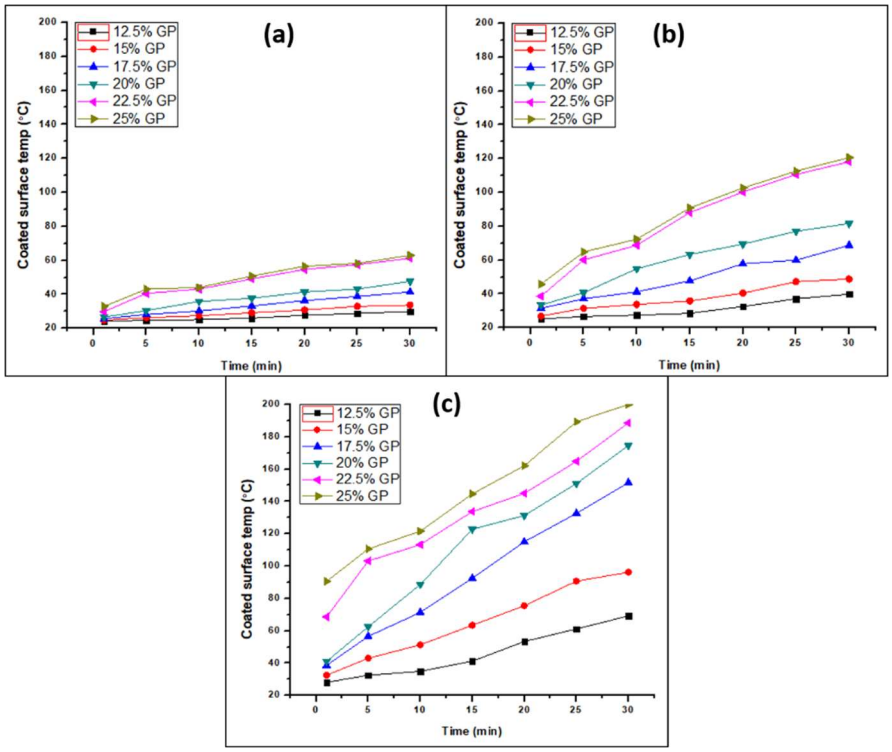

Figure 19: EP-GP coated surface temperature increase vs time with different content of GP (Vol.%) at supply power (a) 10V (b) 20V (c) 30V.

It was also discovered that the EP-GP coated surface exhibited the features mentioned above when the coating surface was subjected to voltages of 10, 20, and 30V. According to the

surface resistivity results of the EP-GP coating for testing heating capacity while supplying voltages, the GP contents doses of 12.5, 15, 17.5, 20, 22.5, and 25% vol. were selected for use in the measurements. The results reveal a trend toward raising the average surface temperature as well as increasing the amount of GP in the composite and the voltage used in the experiments. A considerable change in surface heating was seen at 20V and 30V when 12.5% GP was included in the composite. Within 30 minutes, the average surface temperature increased by 10.1°C, 25.1°C, and 72.6°C for GP concentrations of 15% at 10V, 20V, and 30V, respectively. Comparatively, when the GP content was 17.5% of the total composite, considerable surface heating was detected at temperatures of 17.8°C, 45.1°C, and 128°C. However, excessive spot heating has been seen in the experiment record when the GP concentration is greater than 20%. It was also discovered that when used 25% of GP, the surface temperature of the EP-GP based composite reaches 200°C and starts to burn, a situation that was demonstrated by a 30 voltage power supply was observed. As a result, 25% of the GP content in the EP-GP based coating was removed for further analysis. Figure 19 depicts the surface temperature rising performance of each EP-GP with GP volume contents ranging from 12.5, 15, 17.5, 20, 22.5, and 25%, respectively.

Since these composite coatings are intended to be used concrete pavement surface in cold regions, so get the real field idea that the frozen specimen has been tested for surface heating elevation. The surface heating capacity was investigated of WPU-GP specimens when it was exposed below the freezing temperature at -17°C. Therefore, 15, 17.5, 20, 22.5, 25, and 27.5% GP contains coating was tested by supplying 20V and 30V. Figure 20 shows that above 20% GP containing coating composite demonstrated the required surface temperature rising after 30

minutes.

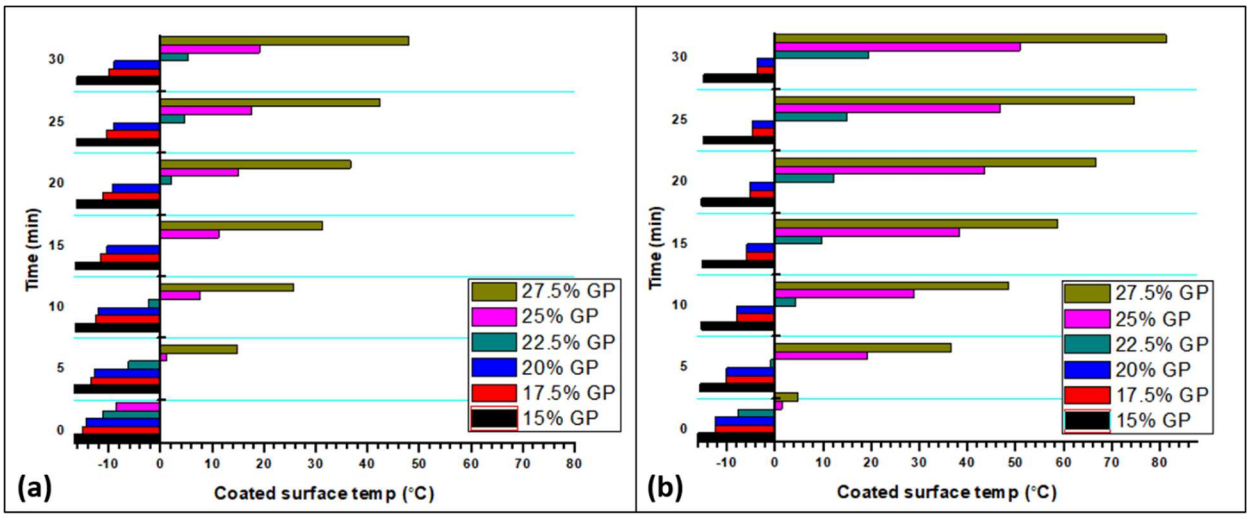

Figure 20: WPU-GP average surface temperature rise at different duration with different voltages (a) 20V, (b) 30V.

The surface heating capacity of the frozen EP-GP composite coating specimens was also tested when their initial temperature was -17°C. During the experiment, the power supplies were tested at 20V and 30V for 30 minutes each to assess the heating capacity of the prepared specimens. Figure 21 illustrates that, when using a 20V power source for 30 minutes, all coating composite surfaces, with the exception of 12.5% GP contents coating, reached temperatures above freezing. On the other hand, all coating composites attained temperatures above freezing after 30 minutes, although 25% of the GP content composite burnt as a result of the higher

temperature present.

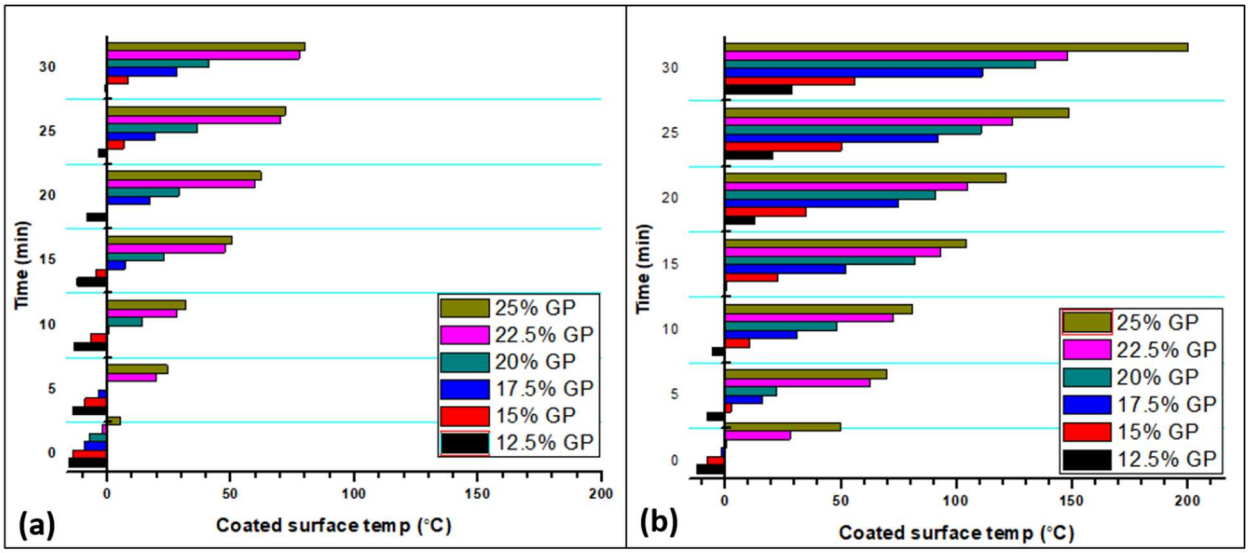

Figure 21: EP-GP average surface temperature rise at different duration with different voltages (a) 20V, (b) 30V.

When GP dose rates are 12.5 percent or higher, as previously indicated, the EP-GP composite exhibits exceptional surface heating capacity; on the other hand, when dose rates are larger than 15 percent, the WPU-GP composite exhibits significant surface heating capability. However, the temperature distribution across two electrodes was even as high as 22.5 percent GP consumption in WPU-GP composites and 20 percent GP usage in EP-GP composites, with no evidence of severe heating in any one area of the composites. GP content was more than 22.5 percent while the amount of heat energy produced from electrical energy was lower. Only a few areas of the covered surface were heated, while the rest of the surface remained unheated in other areas. Agglomeration occurs in composites when graphite powder is poorly distributed in the matrix, and this was observed above the graphite powder content of 22.5 percent. The higher doses of GP, as well as poorly dispersed and uneven surface resistivity, are responsible for the temperature fluctuation on coated surfaces. Regarding surface heating efficacy and distribution,

the appropriate GP content for the WPU-GP is greater than 17.5 percent but not more than 25 percent, according to tests. The EP-GP composites with a GP concentration of 12.5 to 22.5 percent can be used as coating in constructing conductive pavements.

4.3 Experimental Results

Here are six factors that influenced the rise in surface temperature of testing specimens, including the amount of GP in the composite, the thickness of the coating, the spacing between the coatings, the voltage applied, types of specimen, and composite types shown in Figure 22. In order to investigate the measurement of heat conduction effect on specimens while applying coating with conductive composite, GP contents in the amounts of 12.5, 15, 17.5, 20, 22.5, and 25% were chosen for investigation. The temperature changes behavior of the specimen exposed surface and the sandwich top surface were tested during 30, 40, 50, and 60V applied on specimens for 1hr. The investigation revealed that the surface temperature of exposed and sandwich specimens increased gradually with increasing GP fraction volume in the conductive composite, coating thicknesses, voltages, and lowering coating spacing, all of which were done in a stepwise manner.

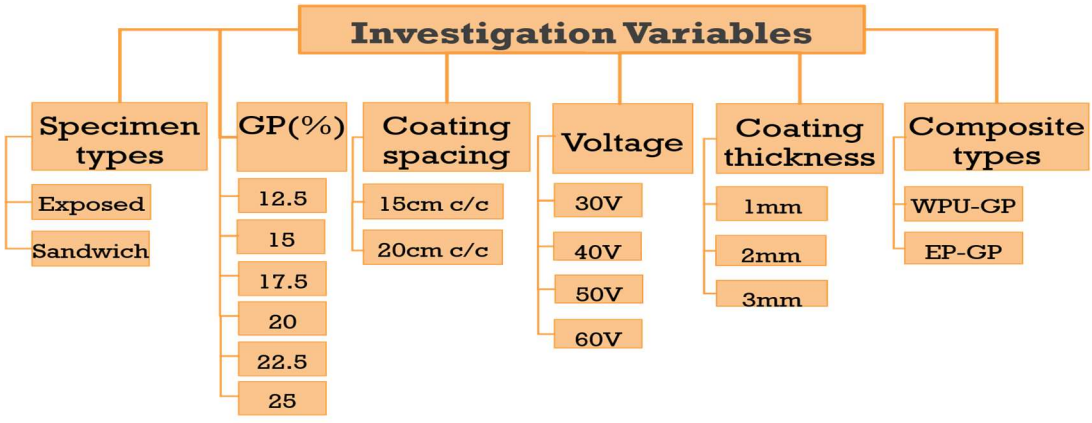

Figure 22: Investigation variables considered in this study.

4.3.1 WPU-GP.

4.3.1.1 Surface temperature measurement.

Figure 23 Figure 24 Figure 25 and Table 8 presents that at room temperature (23.6°C), after the supplied voltage at 40v for 1hr, the surface temperature was measured for both types of specimens exposed and sandwich. The surface temperature of specimens significantly increased after 1hr energized at GP contents 22.5%, for exposed specimens temperature increased (27.5-106%) while temperature increasing decreased for sandwich 8.77-70.55% when strips distance keep at 15cm c/c. In contrast, the temperature rising decreased for both specimen types, such as exposed (6.35-78.09%) and sandwich (2.97-55.85%) when the spacing was increased to 20cm c/c.

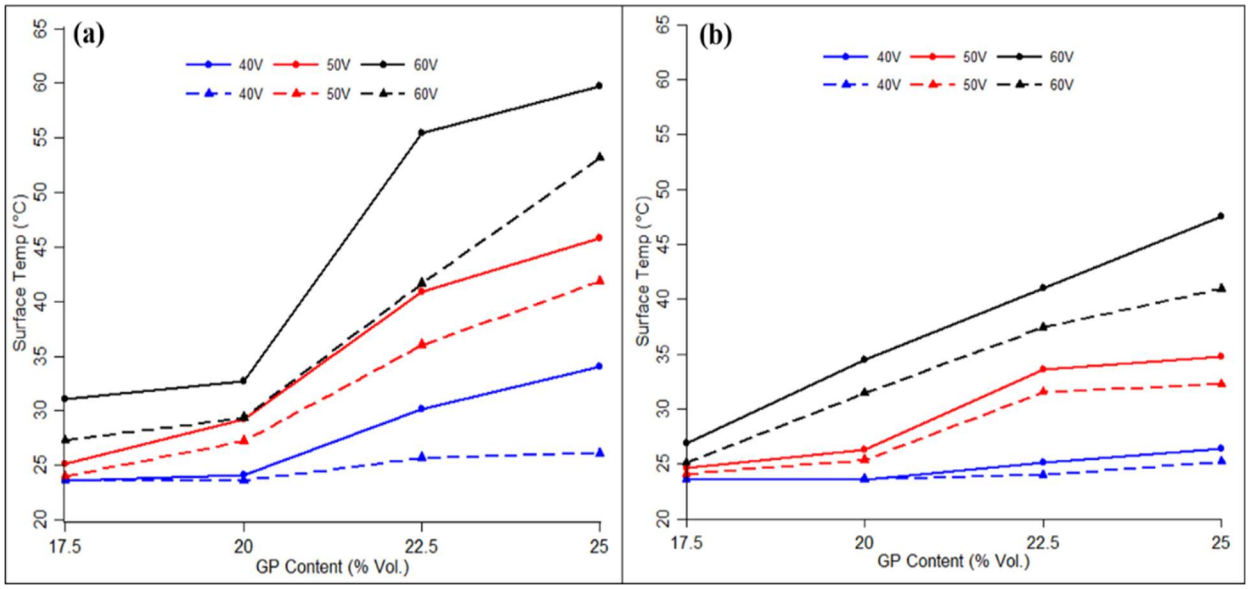

Figure 23: Heat conduction effect of WPU-GP conductive composite strips at a thickness of 1mm while coating spacing (a) 15cm c/c (b) 20cm c/c.

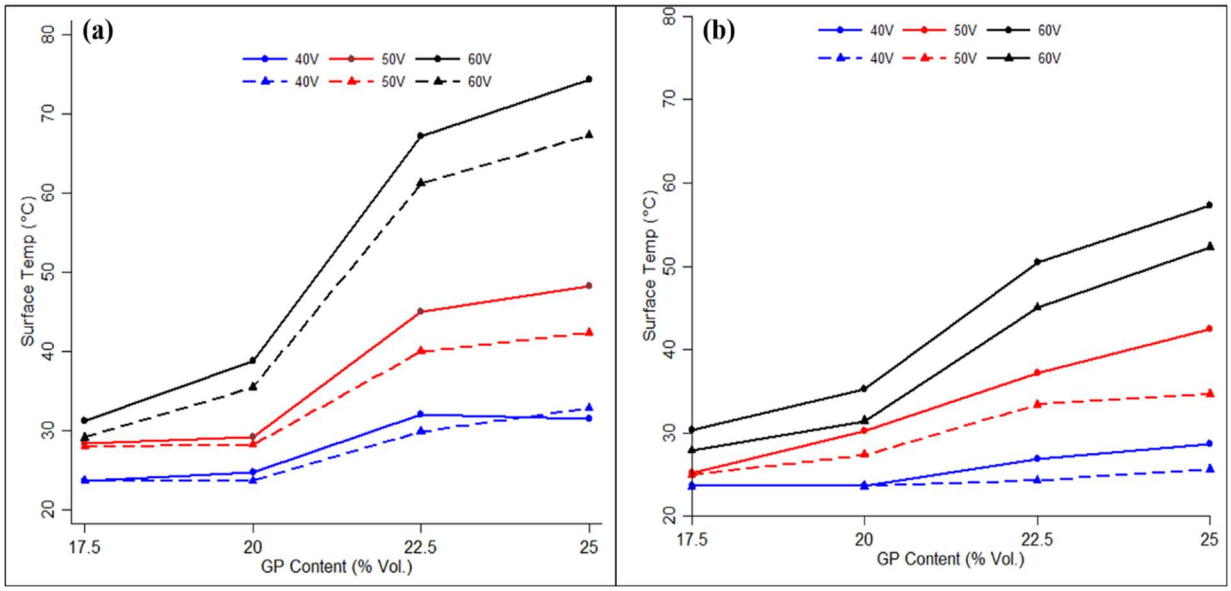

Figure 24: Heat conduction effect of WPU-GP conductive composite strips at a thickness of 2mm while coating spacing (a) 15cm c/c (b) 20cm c/c.

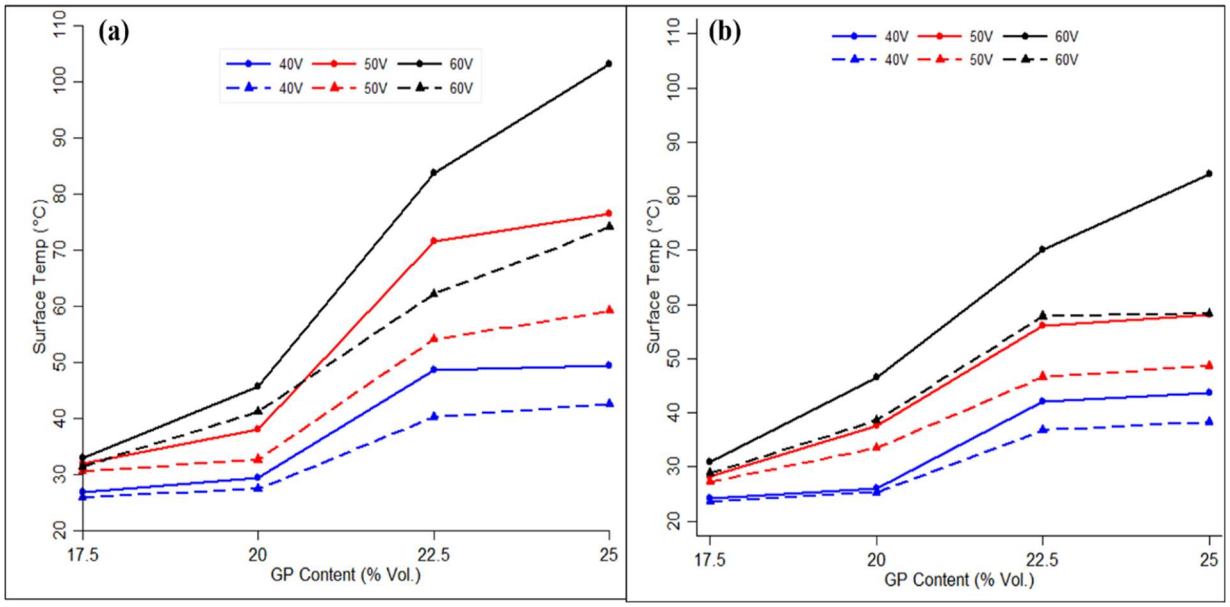

Figure 25: Heat conduction effect of WPU-GP conductive composite strips at a thickness of 3mm while coating spacing (a) 15cm c/c (b) 20cm c/c.

It was observed that the thickness of the coating increased, the surface temperature increased gradually, and a better temperature was observed at 3mm coating thickness. On the other hand, GP contents at 17.5 and 20% of the surface temperature rising were minimal, and the heat conduction effect was not significant to be noted. The GP contents when increased to 25% in the composite, the surface temperature rising increased gradually as for exposed specimens (44.24-109.4%), sandwich (10.7-80.3%) at spacing 15cm c/c, and for 20 cm c/c the temperature rising were measure exposed (11.86-85.42), and for the sandwich (6.78-62.08%). Therefore, the recommended GP content in the conductive composite is 22.5% at 40V.

Table 8: Surface temperature increasing rate test results of the conductive coating after 1hr at 40V.

Gp contents (%)	Surface temperature increase range (°C) after 1hr at 40v													
	Specimen Type	Exposed						Sandwich						
	Spacing C/C (cm)	15			20			15			20			
	Coating Thickness (mm)	1	2	3	1	2	3	1	2	3	1	2	3	
17.5	Temperature Changes (°C)	0	0	3.32	0	0	0.5	0	0	2.37	0	0	0	
20		0.5	1.1	5.87	0	0	2.5	0	0	3.82	0	0	1.7	
22.5		6.5	8.4	24.9	1.5	3.32	18.4	2.07	6.22	16.6	0.4	0.7	13.1	
25		10.4	7.9	25.8	2.8	5.1	20.1	2.52	9.21	18.9	1.6	2.07	14.6	

According to Table 9, under different GP contents in the composite, the investigation for surface temperature increasing by heat conduction effect of used conductive composite strips at different spacing and thickness of both types of specimens measure at 50v for 1hr energization. Table 9 shows that at GP contents 17.5% and 20%, the temperature rising is greater than 40V electrifying. The temperature increase was higher, observed at GP contents 22.5% when spacing

was 15cm c/c surface temperature increased exposed (73.35-203.4%), sandwich (52.6-129.2%), whereas at spacing 20 cm c/c the temperature rising was decreased for exposed (42.29-137.9%), and sandwich (33.64-97.42%). The GP contents increased to 25%, the surface temperature rising was very high after 1hr for 50V application. However, considering the GP contents 25% in the composite, they start to melt and burn during 1hr current application. Therefore, the GP contents 25% are not recommended to use in the composite since voltage application near 50V started burning and observed some micro-cracks after achieving full curation.

Table 9: Surface temperature increasing rate test results of the conductive coating after 1hr at 50V.

Gp contents (%)	Surface temperature increase range (°C) after 1hr at 50v											
	Specimen Type	Exposed						Sandwich				
	Spacing C/C (cm)	15			20			15			20	
	Coating Thickness (mm)	1	2	3	1	2	3	1	2	3	1	2	3
17.5	Temperature Changes (°C)	1.5	4.8	8.36	1	1.6	4.7	0.4	4.3	6.98	0.5	1.4	3.6
20		5.62	5.49	14.38	2.73	6.67	14.03	3.61	4.56	9.07	1.75	3.75	9.89
22.5		17.31	21.45	48	9.98	13.6	32.55	12.41	16.37	30.48	7.94	9.8	22.99
25		22.2	24.63	52.87	11.18	18.9	34.52	18.25	18.72	35.54	8.65	11.07	25.08

The investigation method for the heat conduction effect of conductive composite used as parallel strips at 60V as same as the above-mentioned procedure. The specific test results are shown in Figures 25, 26, and 27. Where reported that at an ambient temperature of 23.6°C, with power supply 60V, the surface temperature increase was measured after 1hr energized. The surface temperature of exposed specimens increased by (31.53-39.24%), and sandwich (15.7-

33.22%) when GP content was 17.5%, and spacing was considered 15cm c/c, whereas temperature increasing slightly decreased for spacing 20cm c/c such as exposed (13.86-30.93%), and sandwich (6.441-22.03%). The expected results were observed at GP contents 20% in the composite, for exposed temperature increased by (46.23-97.46%) and sandwich (24.4-74.58%) at spacing 15cm c/c, however using spacing 20cm c/c temperature increasing most likely similar though the increasing spacing between strips, for exposed increased by (38.52-93.52%), and sandwich (33.22-63.39%). At voltage 60V, using GP contents more excellent than 20%, such as 22.5 and 25%, observed conductive composite started melting and burnt since producing high temperature by conductive composite. Hence, from the perspective of heat conduction efficiency and considering the economic condition of pavement construction, the recommended GP contents in the composite are between 20-22.5%.

Table 10: Surface temperature increasing rate test results of the conductive coating after 1hr at 60V.

Gp contents (%)	Surface temperature increase range (°C) after 1hr at 60v												
	Specimen Type	Exposed						Sandwich					
	Spacing C/C (cm)	15			20			15			20		
	Coating Thickness (mm)	1	2	3	1	2	3	1	2	3	1	2	3
17.5	Temperature Changes (°C)	7.44	7.63	9.26	3.27	6.7	7.3	3.7	5.49	7.84	1.52	4.28	5.2
20		10.9	11.6	23	9.09	15.2	22.0	5.75	11.8	17.6	7.84	7.83	14.9
22.5		31.8	43.5	60.1	17.4	26.8	46.4	18.0	37.6	38.5	13.8	21.4	34.2
25		36.1	50.7	79.5	23.9	33.7	60.4	29.5	43.7	50.4	17.3	28.7	34.7

4.3.1.2 Recorded duration for reaching 0°C temperature of specimens.

Figure 26 shows the relationship between time requirements and Gp contents to achieve 0°C temperature of specimens while the ambient temperature was -17°C. The needed time decreases for both types of specimens while the GP concentrations and coating thickness increase, as shown in Figure 26. Increasing GP volume fraction from 17.5% to 20% resulted in reducing time requirement at different coating thicknesses. This trend was observed most at coating thickness 3mm for both specimens when the spacing was maintained at 15cm c/c.

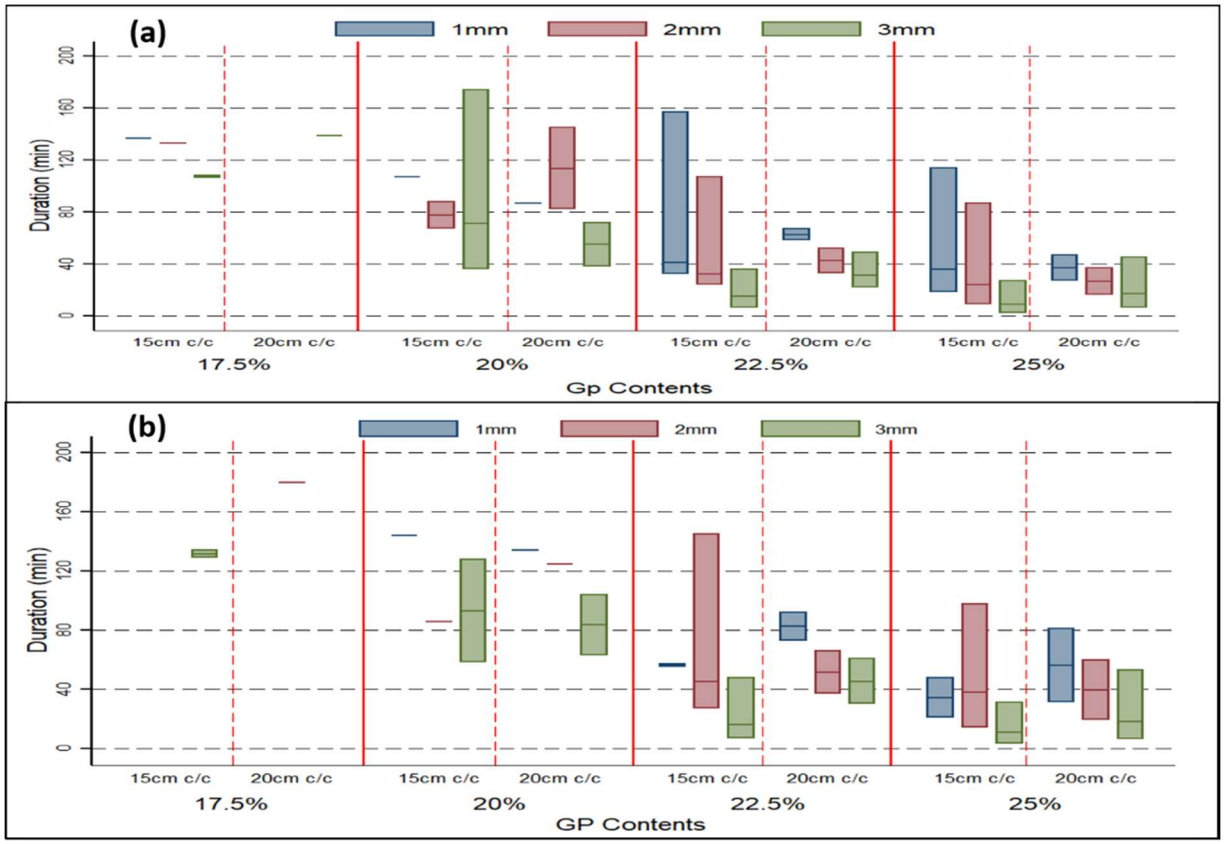

Figure 26: The heating performance of the used construction method at below-freezing temp (a) exposed (b) sandwich.

It was discovered that a few specimens with GP contents of 17.5 and 20% were capable of eliminating the negative temperature shown. In contrast, at 22.5 and 25% GP dosage rates, the

temperature of all specimens reached 0°C from -17°C, which was found to be a statistically significant outcome of this study. As seen in Figure 26 there was a substantial drop in the time requirement at the GP volume fraction of 22.5 and 25%, which corresponds to the spacing of coating 15 and 20cm c/c of both types of specimens. This finding indicates that a higher content of GP with a greater thickness contributes to the production of resistive heating of the conductive composite when a higher power supply is applied. That reduces the time required for the testing specimen to reach a surface temperature of 0°C when exposed to a -17°C environment.

4.3.2 EP-GP.

4.3.2.1 Surface temperature measurement.

The surface temperature of both types of exposed and sandwich specimens was recorded at room temperature (23.6°C) after a 1hr supply voltage of 30v, as shown in Figure 27 and Table 11. After 1 hour of energizing at 20% GP, the surface temperature of exposed specimens increased (123.1-145.8%), whereas the temperature of sandwich specimens reduced (78.9-137.5%) when strips distance was kept at 15cm c/c. When the spacing was extended to 20cm c/c, however, the temperature increased somewhat lowered for both exposed (106.6-131.8%) and sandwich (93.7-113.1%) specimen types. The surface temperature gradually improved as the coating thickness increased, with a better temperature being reported at 3mm coating thickness. Though the temperature increases well at 20% GP, the composite application on the specimen was difficult due to the high viscosity of the composite at higher percentages of GP. The same temperature rises were seen at GP amounts of 22.5 percent, however due to the high viscosity of the composite, it could not be used on the specimen. GP contents, on the other hand, were insignificant at 12.5 and 15% of the surface warming, and the heat conduction effect was not significant enough to be noticed. When the GP content in the composite was increased to 17.5

percent, the surface increases up gradually as for exposed specimens (53.1-131.1%), sandwich (45.2-103%) at spacing 15 cm c/c, and for 20 cm c/c the temperature climbed as recorded exposed (47.9-91.4%) and sandwich (45.2-103%). As a result, at 30V, the recommended GP content in the conductive composite is 17.5 percent, which met both the temperature increasing efficiency and the practical application on the specimen.

Table 11: Surface temperature increasing rate test results of the conductive coating after 1hr at 30V.

Gp contents (%)	Surface temperature increase range (°C) after 1hr at 30v												
	Specimen Type	Exposed						Sandwich					
	Spacing C/C (cm)	15			20			15			20		
	Coating Thickness (mm)	1	2	3	1	2	3	1	2	3	1	2	3
12.5	Temperature Changes (°C)	2.56	5.	7.	1.	2.	3.	1.	5	5.	0.	1.	2.
15		9.	15	16	6.	7.	9.	8.	12	15	5.	6.	6.
17.5		12	21	30	11	20	22	10	15	24	10	13	17
20		29	29	34	25	28	31	18	26	32	22	22	26
22.5		29	40	41	28	38	41	23	28	40	27	28	38

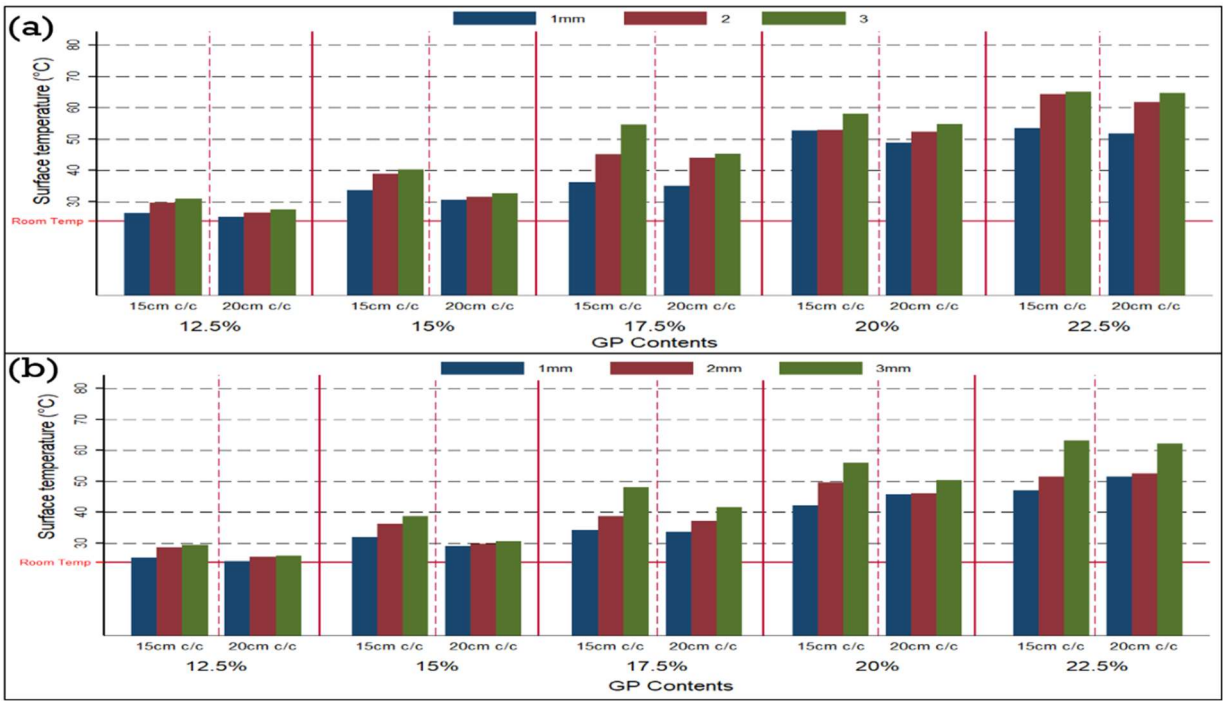

Figure 27: Heat conduction effect of EP-GP conductive composite strips while supplying voltage 30V for 1hr (a) exposed (b) sandwich.

Table 12 shows the surface temperature rise by heat conduction effect of applied conductive composite strips at varied spacing and thickness of both types of specimens determined at 40v for 1hr energization. Figure 28 shows that for GP concentrations of 12.5 percent and15%, respectively, temperature increases greater than 30V electrifying. According to Figure 28, the temperature increased sharply for both specimens at 15cm c/c when the GP was 15%, but only marginally when the spacing was increased to 20cm c/c. At 17.5% GP contents, when the spacing used 15 cm c/c, the temperature was raised higher for exposed (111.1-258.1%) and sandwich (95.6-172.5%), whereas when the spacing was 20 cm c/c, the temperature goes up less for exposed (88.1-170.2%) and sandwich (95.6-172.5%). As a result, at 17.5 percent GP content, both specimens and coating spacing experienced a higher temperature increase. After 1 hour of 40V application, the GP content increased to 20%, and the surface temperature reached a

peak. Even though the composite contains 20% GP provided higher surface temperature rising, it begins to melt slowly and burns before the current application cycle of 1 hour is completed. Also 22.5 percent GP content could not withstand 40 V, it was burned within minutes of reaching its melting point. As a result, GP contents of 20 and 22.5 percent are not suggested for use in composites while voltage applications near 40V since they were started burning.

Table 12: Surface temperature increasing rate test results of the conductive coating after 1hr at 40V.

Gp contents (%)	Surface temperature increase range (°C) after 1hr at 40V											
	Specimen Type	Exposed						Sandwich				
	Spacing C/C (cm)	15			20			15			20	
	Coating Thickness (mm)	1	2	3	1	2	3	1	2	3	1	2	3
12.5	Temperature Changes (°C)	4.73	10.7	12.07	2.41	4.28	6	3.7	8.06	9.5	0.9	2.37	3.1
15		17.3	35.7	39.85	8.65	11.8	15	14.9	23.1	30	8.63	9.42	12.71
17.5		26.22	46.7	60.9	20.78	31.1	40	22.55	29.7	41	16.19	16.83	33.99
20		66.6	77.8	87.85	40.12	47.4	52	56.18	59.6	75	25.83	40.24	41.03
22.5		Coating burned											

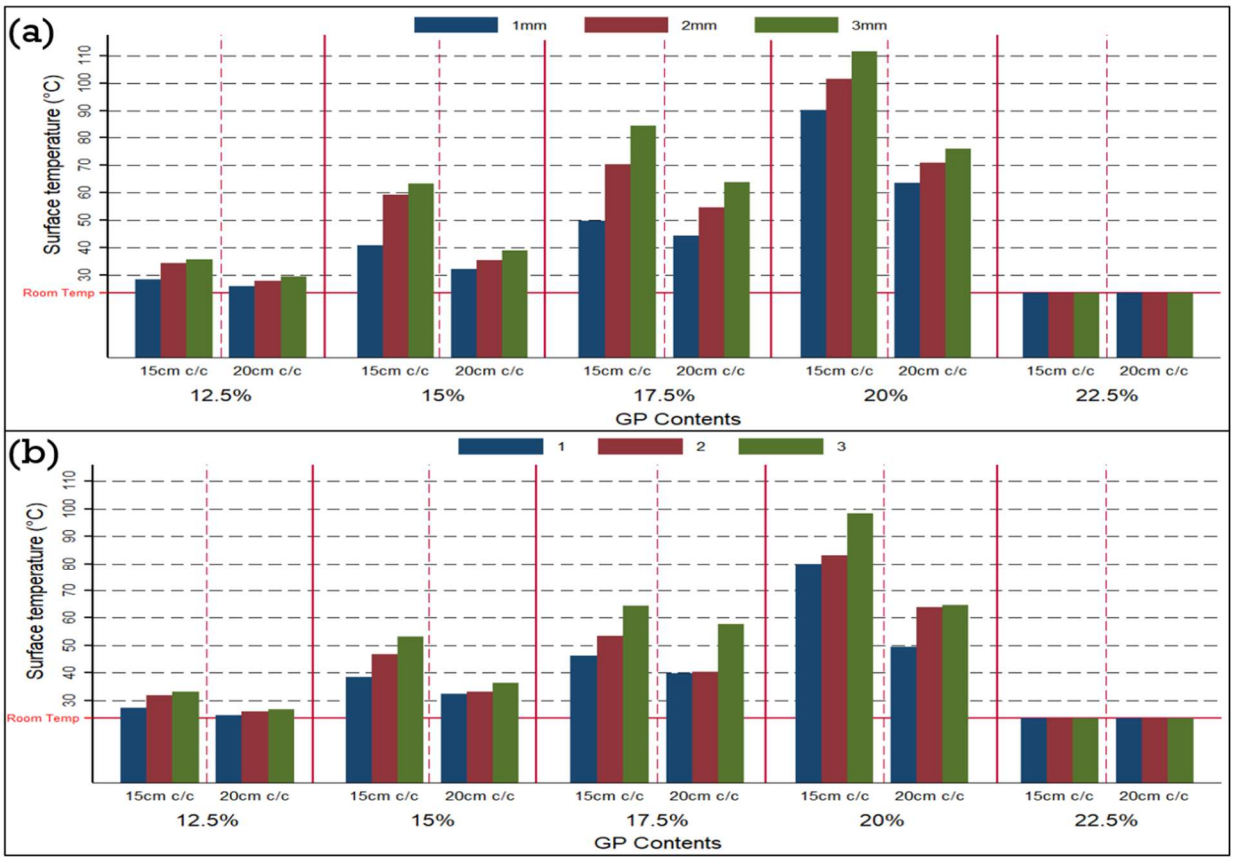

Figure 28: Heat conduction effect of EP-GP conductive composite strips while supplying voltage 40V for 1hr (a) exposed (b) sandwich.

The same method was utilized to investigate the heat conduction effect of conductive composite strips at 50V. Figure 29 and Table 13 show the results of the specific tests. The surface temperature increased after 1 hour of power at 23.6°C ambient temperature with 50V power supply. When the GP content was 12.5 percent and the spacing was 15cm c/c, the surface temperature of exposed specimens increased (54.4-150.3%) and sandwich (31.8-116.9%), whereas temperature increased marginally for spacing 20cm c/c for exposed (23.3-62.3%), and sandwich (18.2-29.8%). At GP content 15%, it was found that exposed temperature increased by (109.4-211%) and sandwich temperature increased by (64.2-187.3%) at spacing 15 cm. However, spacing 20cm c/c temperature increasing is most likely similar though the increasing

spacing between strips, for exposed increased by (80.8-138.5%), and sandwich (46.7-114.8%). At voltage 50V, using 17.5% GP contents more excellent than 15%, where observed at 15cm c/c for exposed (207-315.7%) and sandwich (152.5-231.4%), when spacing increased to 20 cm c/c temperature increased for exposed (160.6-274.9%) and sandwich (112.4-178.6%). A 20% increase in GP concentration caused high temperature melting and burning of the applied conductive composite. The suggested GP content in the composite is between 15-17.5 percent for heat conduction efficiency and the economic situation of pavement construction.

Table 13: Surface temperature increasing rate test results of the conductive coating after 1hr at 50V.

Gp contents (%)	Surface temperature increase range (°C) after 1hr at 50V											
	Specimen Type	Exposed						Sandwich				
	Spacing C/C (cm)	15			20			15			20	
	Coating Thickness (mm)	1	2	3	1	2	3	1	2	3	1	2	3
12.5	Temperature Changes (°C)	12.84	18	35.61	5.51	7.55	15	7.5	13.1	28	4.29	4.62	7.03
15		25.81	37.7	49.8	19.07	26.1	33	15.14	32	44	11.02	14.51	27.06
17.5		48.95	60.8	74.5	37.9	45.7	65	36	45.6	55	26.52	36.06	42.16
20		Coating burned											
22.5													

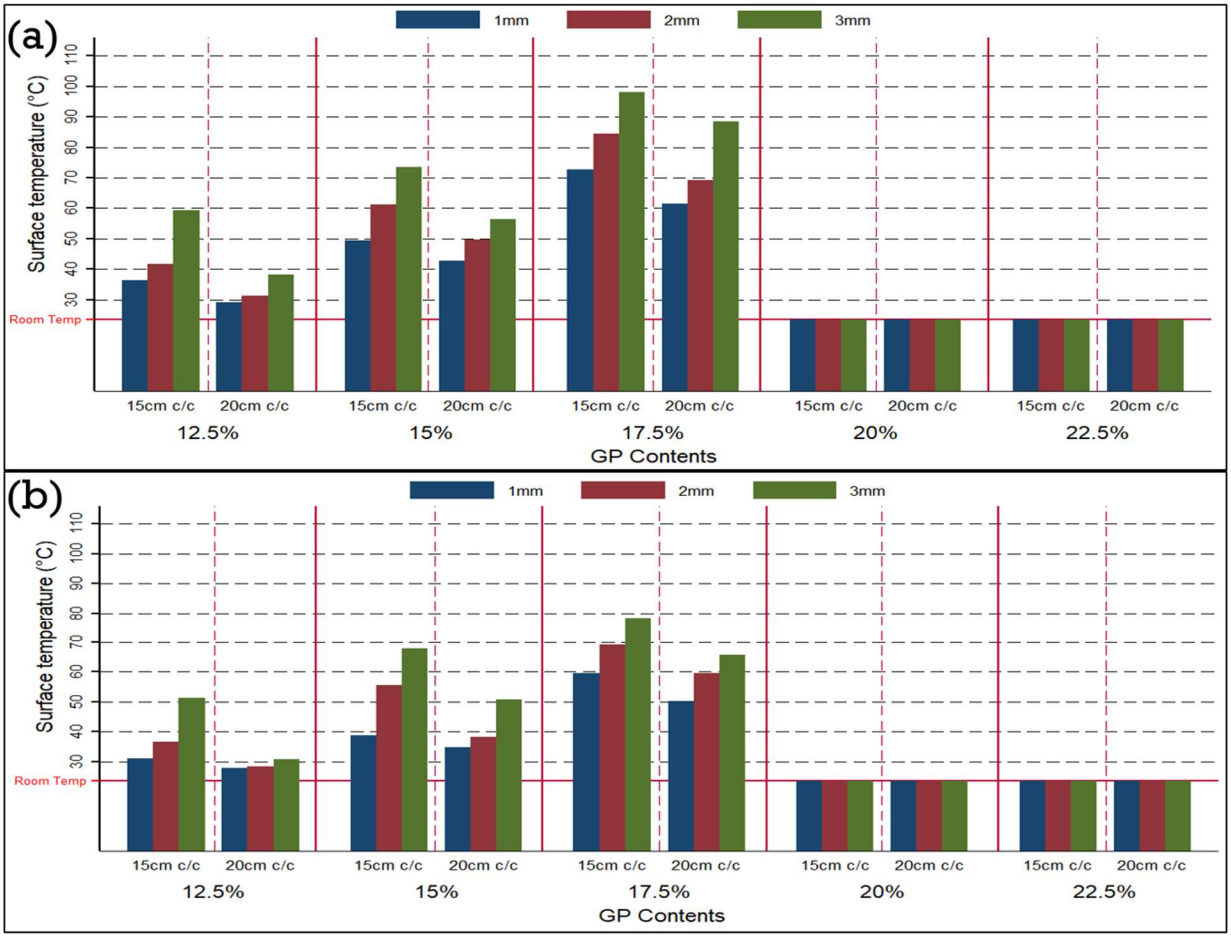

Figure 29: Heat conduction effect of EP-GP conductive composite strips while supplying voltage 40V for 1hr (a) exposed (b) sandwich.

4.3.2.2 Recorded duration for reaching 0°C temperature of specimens.

Figure 30 requirements and Gp contents to obtain a temperature of 0°C for specimens at -17°C ambient temperature. As the GP concentrations and coating thickness increase, the required mean time reduces for both types of specimens, as illustrated in Figure 30. When the spacing was kept at 15cm c/c, and the coating thickness was 3mm for both specimens, this tendency was most noticeable. All specimens with GP concentrations above 15% were found to have attained temperatures above 0C, as indicated in Figure 30. Increasing the GP volume fraction from 12.5 percent to 15 percent with various coating thicknesses and spacing reduced the mean time

requirement. At 15% GP contents, the mean time requirements vary depending on the coating spacing and thickness. For example, the 15 cm c/c coating spacing required to meantime were between (75-25 min), whereas the 20 cm c/c required a mean time of (75-25 min) for both exposed and sandwich specimens. The temperature of all specimens reached 0°C from -17°C at 17.5 percent GP dosage rates, and the recorded meantime for both specimens was between 75 and 25 minutes at 15 and 20 cm c/c, which was shown to be a notable effect of utilizing EP-GP composite. As shown in Figure 30, the time required for the GP volume fractions of 20 and 22.5 percent, which correspond to coating spacing of 15 and 20cm c/c of both types of specimens, was significantly reduced. This finding suggests that when a higher power supply and coating thickness is used with a larger concentration of GP adds to the formation of resistive heating of the conductive composite.

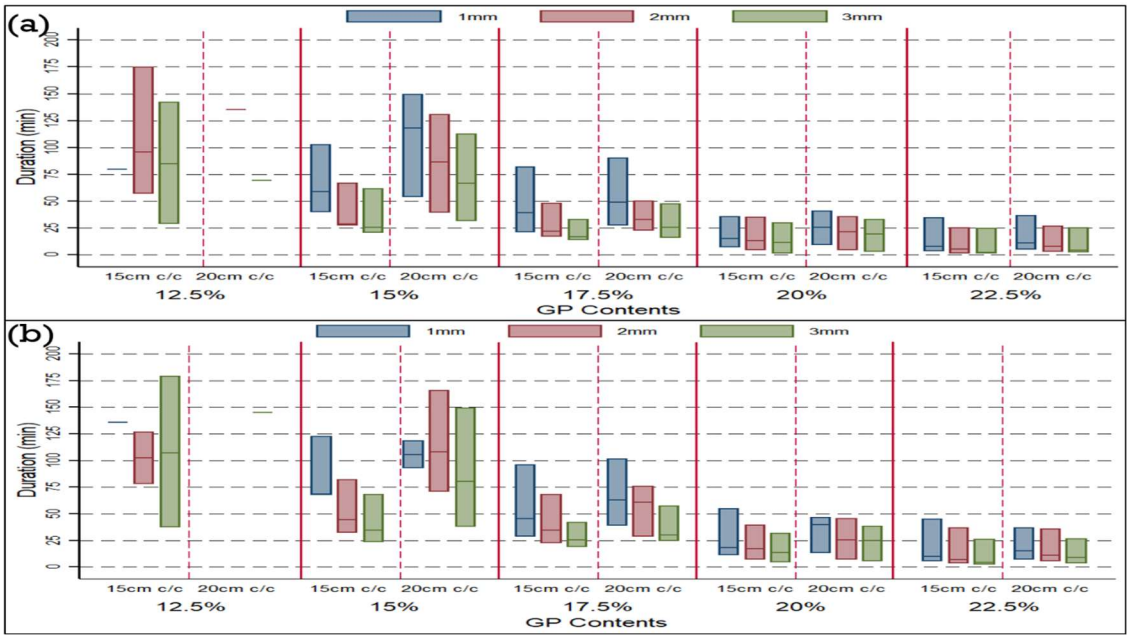

Figure 30: The heating performance of the EP-GP composite at below-freezing temp (a) exposed (b) sandwich.

4.4 Discussion

The study proposed a construction method for electrically conductive pavement, where utilized electrically conductive coating composite as a heating element and purpose to reduce resource costs while offering good heating efficiency, allowing snow and ice to melt from pavements. As a result, a comprehensive investigation was conducted to assess the heat conduction impacts of used two composite such as WPU-GP, and EP-GP. In the investigation GP contents at varied concentrations of 12.5, 15, 17.5, 20, 22.5, and 25% with increasing thicknesses of 1, 2, and 3mm, and supplied AC voltages of 30, 40, 50, and 60V. The results of exposed and sandwich specimens were compared, with coating spacing varied between 15cm and 20cm c/c. On the basis of the experimental purposes, the analysis method can be divided into two aspects: the final surface temperature at room temperature and the time required for testing specimens to reach 0°C after being cooled from -17°C temperature. The study included 648 specimens, with 324 being evaluated at room temperature and 324 being tested below freezing temperature. The analysis was performed to compare the mean temperature rising between two composites heating performance. The results showed that the presence of 20% GP content in the WPU-GP based coating resulted in a higher surface temperature rise when compared to the presence of 17.5% GP content. The heat conduction effect was greatly enhanced by increasing the GP content from 20 to 22.5% of the composite's volume, however, the mean temperature did not improve significantly by increasing the GP content from 22.5 to 25%. To enhance surface temperature while keeping GP content within the required range, 20 to 22.5 percent GP is

recommended for the WPU-GP based coating, and Figure 31 represents their results.

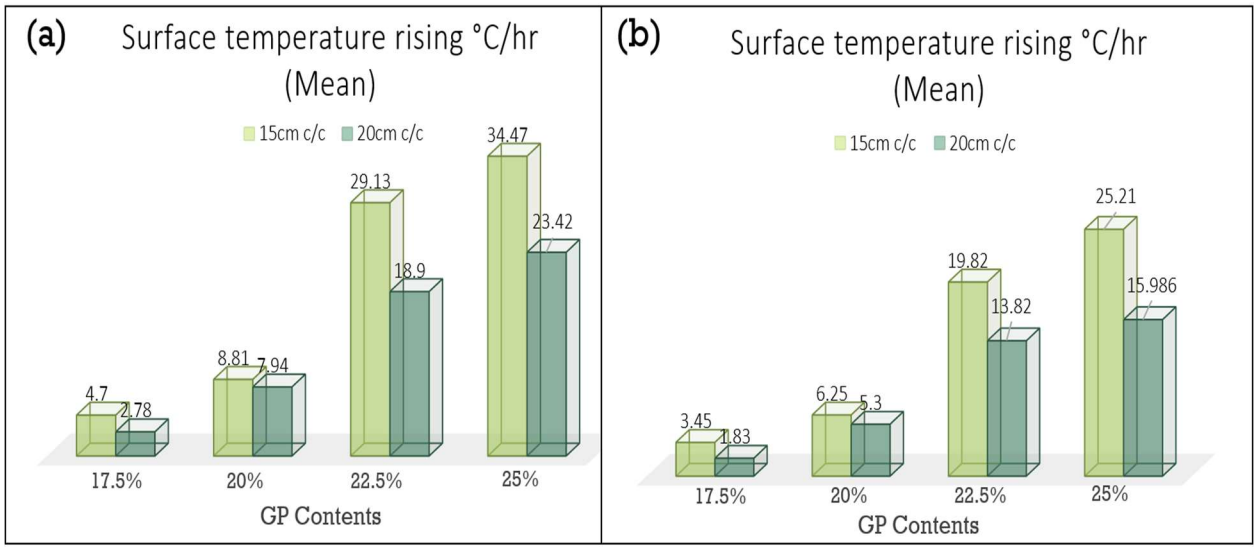

Figure 31: Mean surface temperature rising °C/hr of WPU–GP based construction method (a) exposed (b) sandwich.

The EP-GP based construction method's mean surface temperature range is shown in Figure 32. The results demonstrate that the EP-GP based coating with 15% GP content had a higher surface mean temperature than the coating cmposite with 12.5% GP content. When the EP-GP content is increased from 15 to 17.5 percent of the composite's volume, the heating impact is observed to be greater than when the GP content is 12.5 and 15 percent. The mean temperature increasing GP content from 20 to 22.5 percent was not included in the presentation

since those composites were deemed unsafe for using as coating material.

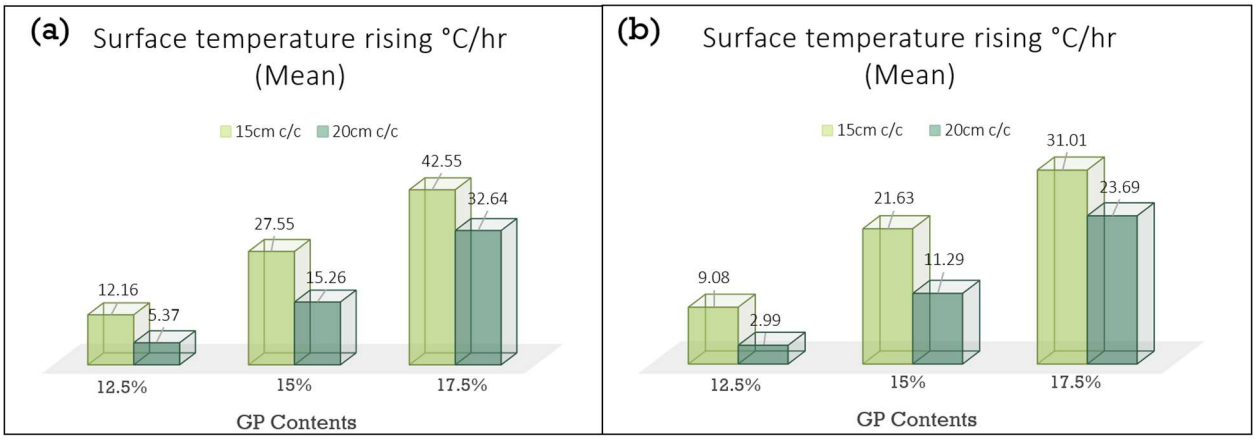

Figure 32: Mean surface temperature rising °C/hr of EP–GP based construction method (a) exposed (b) sandwich.

Since coating composite is used in parallel strips on the specimen surface, Figure 33 indicates employing a WPU-GP and EP-GP composites configuration to construct a more sustainable approach with lower cost. That allows for significant cost savings over conventional conductive composite coatings. Following extensive evaluations of this construction method's economical cost and heating performance, using 22.5% GP content in the WPU-GP, and 17.5% GP for EP-GP based coating is recommended for lower material use.

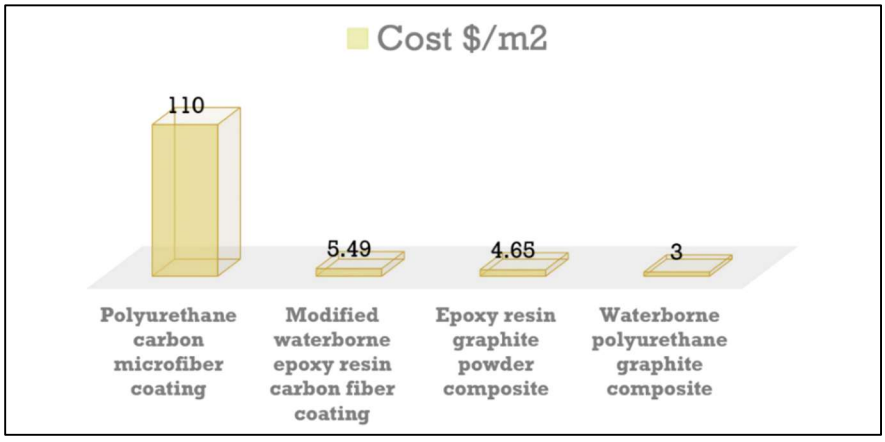

Figure 33: The construction cost of different conductive composite coating.

Also included is a technical advantage of the proposed construction method, which is shown in Figure 34 to help illustrate its functional efficiency. The experimental outcome of the used construction method is shown in Figure 34 compared to other existing deicing technologies (Lai, Liu, and Ma 2014). Figure 34 shows that the construction method outperforms other deicing technologies such as carbon fiber grills, electrical heating grids, conductive heating cables, and conductive concrete in terms of heating efficiency. Consequently, it was concluded that the construction approach had enhanced the surface temperature of PCC specimens, implying that this construction method might be used for Electrically Conductive Pavement construction.

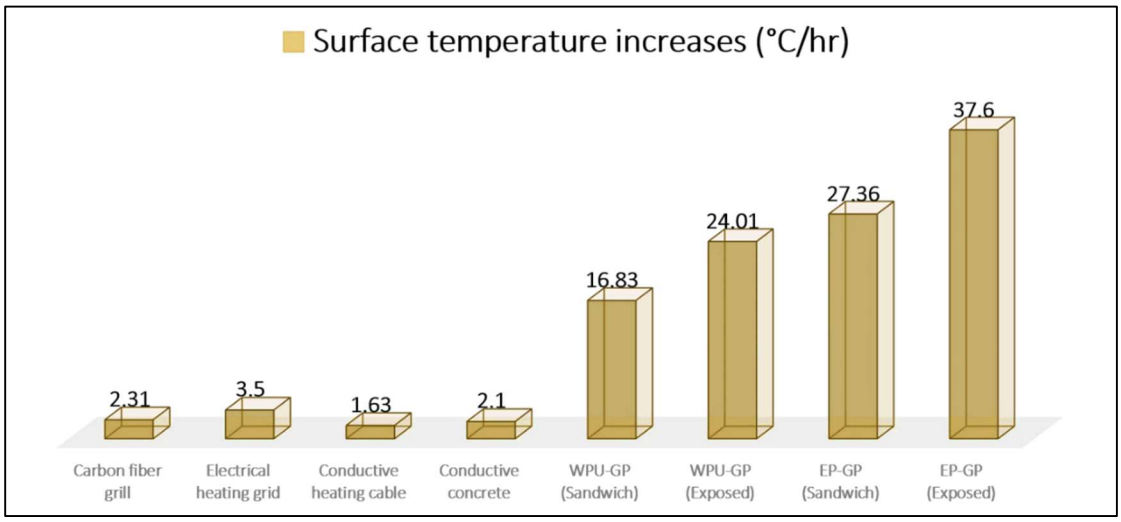

Figure 34: Surface temperature rising rates per hour for various methods of electrical heating pavement systems.

CHAPTER V

CONCLUSIONS

This article proposed a more sustainable construction method for electrically conductive pavement in which electrically conductive coating composite is used as a heating element for heating the pavement surface. It is constructed utilizing the coating composite following a parallel striping approach with two coating distances specified in the system design. Based on PCC specimen heat and construction costs, the studies evaluated the results, which demonstrated that the construction method combined with a noble strategy provided sufficient resistive heating to keep the surface temperature of the specimen above freezing. This enables specimen surfaces to be heated to varying ambient temperatures and compares the findings for both exposed and sandwiched samples. The optimal 22.5% GP of WPU-GP and 17.5% of GP content in the EP-GP composite is deemed the optimal coating composite heating material. It results in an average temperature increase of 71.3% for the sandwich a 101.74% increase on the exposed specimen surface at room temperature when using WPU-GP composites. In contrast, the EP-GP based construction method provides more heating efficiency, such as 115.9% for the sandwich and 159.3% for the exposed specimen. Concerning cost, it has been demonstrated that the proposed construction approach is less expensive to construct than other existing techniques while also providing more significant technological advantages.

The main findings of the investigation can be summarized as:

- The applied composite coating has contained different factions of GP in the WPU and EP matrix determined the percolative behavior of GP in the composite while studying the optimal range of GP. The percolation transition zone of WPU-GP was observed from 17.5% to 25% that also changes composite materials behavior turns to conductive. Other materials behavior such as EP-GP transition zone was noticed in the 12.5%-22.5% GP volume fractions corresponding to transition to conductive composite.
- The resistive heating test was conducted for the WPU-GP composite and showed 17.5% of GP dosages started to show heating capacity slightly, and it was escalated along with the increasing of GP contents. The significant heating efficacy has noticed the range of 20-22.5 % of GP contents in the composite. The use of above 22.5% GP contents in the composite decreases the heating capacity rising regarding average coating surface temperature.
- The EP-GP composite was subjected to a resistive heating test, which revealed that 12.5 percent of GP dosages began to demonstrate heating capacity, which increased as the GP content increased. The range of 15-22.5 percent GP concentration in the composite has shown significant heating efficacy. The addition of 17.5 percent GP to the composite boosts the heating capacity while also raising the average coated surface temperature.
- In order to reduce the amount of coating materials used on PCC specimens, parallel strips were coated instead of the entire surface. Determined strip distance between each other, chose stripe distances of 15 and 20cm c/c and was able to significantly heat uncoated area.
- The study was conducted at two different types of specimens: exposed and sandwich specimens. A 30mm thick concrete layer was placed over the coated surface to protect

the conductive coating materials from abrasion between the vehicle tires and the coated surface.

- The heating performance of the specimen at room temperature continuously increased with rising the fraction volume of GP up to 25%. However, the expected efficiency was achieved at GP contents 22.5%.
- With increasing GP fraction volume, the heating performance of WPU-GP and EP-GP prepared specimens at room temperature improved. At GP contents, the predicted efficiency was 22.5%for WPU-GP and 17.5% for EP-GP.
- For the purpose of determining the heating efficiency of testing specimens, the relationship between GP concentrations, coating thickness, and voltage application was investigated.

5.1 Limitations

Some limitations of this research work are described below:

(1) Due to varying surface resistivity of composites, it is clear that manual mixing was insufficient to establish a uniform mixing of GP in composites, which did not allow for creating well-conductive channels inside the composite, and thus, desired conductivity was not achieved.

(2) Another drawback of the current study was the uneven distribution of coating on the specimen surface. The effect of coating thickness on accuracy cannot be determined in the molding application process because of the random coating thickness.

(3) The real-time data records were not possible with the surface heating measurement device employed in this study. Because infrared heating measures always deliver the temperature of a specific place rather than covering the complete testing surface area,

(4) Despite the fact that this research was conducted in a consistent lab setting that was difficult to regulate due to temperature variations in the surroundings, it allowed the specimens' temperature to rise.

(5) During this research, the construction expenses of a laboratory-sized specimen were studied, and it is possible that these prices will vary while constructing larger-scale field experiments.

5.2 Future Work

Following works are suggested based on the current research work:

(1) To evaluate real-time surface heating temperature, it is advised that future studies employ advanced thermal scan strategies and/or combine other heating measuring methods. This will enable sufficient data recordings to be collected in order to obtain an average surface temperature.

(2) Two parallel strips of coating measuring 150 mm in length and 50 mm in width were used in this study, and they were only considered for the investigation of small size specimens. Adding more strips to the inquiry may provide a better understanding of the heat conduction impact of the specimen surface, which will allow more detail to be obtained.

(3) Field-scale experiments can be conducted to capture the significance of the construction method; hence large-scale experimentation should be studied for future research.

(4) While analyzing the cost of the proposed approach, it is essential to consider both the operating and construction expenses, as this will provide a better understanding of how well this method performs in comparison to other existing approaches.

REFERENCES

[1] S. M. S. Sadati, K. Cetin, H. Ceylan, A. Sassani, and S. Kim, "Energy and thermal performance evaluation of an automated snow and ice removal system at airports using numerical modeling and field measurements," *Sustain. Cities Soc.*, 2018, doi: 10.1016/j.scs.2018.08.021.

[2] J. Wu, J. Liu, and F. Yang, "Three-phase composite conductive concrete for pavement deicing," *Constr. Build. Mater.*, 2015, doi: 10.1016/j.conbuildmat.2014.11.004.

[3] A. Sassani *et al.*, "Carbon fiber-based electrically conductive concrete for salt-free deicing of pavements," *J. Clean. Prod.*, 2018, doi: 10.1016/j.jclepro.2018.08.315.

[4] Y. Farnam, A. Wiese, D. Bentz, J. Davis, and J. Weiss, "Damage development in cementitious materials exposed to magnesium chloride deicing salt," *Constr. Build. Mater.*, 2015, doi: 10.1016/j.conbuildmat.2015.06.004.

[5] H. Wang, C. Thakkar, X. Chen, and S. Murrel, "Life-cycle assessment of airport pavement design alternatives for energy and environmental impacts," *J. Clean. Prod.*, 2016, doi: 10.1016/j.jclepro.2016.05.090.

[6] Y. Farnam, S. Dick, A. Wiese, J. Davis, D. Bentz, and J. Weiss, "The influence of calcium chloride deicing salt on phase changes and damage development in cementitious materials," *Cem. Concr. Compos.*, 2015, doi: 10.1016/j.cemconcomp.2015.09.006.

[7] Y. Farnam, D. Bentz, A. Hampton, and W. J. Weiss, "Acoustic emission and low-temperature calorimetry study of freeze and thaw behavior in cementitious materials exposed to sodium chloride salt," *Transportation Research Record*. 2014, doi: 10.3141/2441-11.

[8] Y. Farnam, D. Bentz, A. Sakulich, D. Flynn, and J. Weiss, "Measuring Freeze and Thaw Damage in Mortars Containing Deicing Salt Using a Low-Temperature Longitudinal Guarded Comparative Calorimeter and Acoustic Emission," *Adv. Civ. Eng. Mater.*, 2014, doi: 10.1520/acem20130095.

[9] L. Sutter, K. Peterson, G. Julio-Betancourt, D. Hooton, T. Van Van Dam, and K. Smith, "The deleterious chemical effects of concentrated deicing solutions on Portland cement concrete," *South Dakota Dep. Transp. Off. Res.*, 2008.

[10] X. Shi, L. Fay, M. M. Peterson, and Z. Yang, "Freeze-thaw damage and chemical change of a Portland cement concrete in the presence of diluted deicers," *Mater. Struct. Constr.*, 2010, doi: 10.1617/s11527-009-9557-0.

[11] A. Sassani, H. Ceylan, S. Kim, A. Arabzadeh, P. C. Taylor, and K. Gopalakrishnan, "Development of Carbon Fiber-modified Electrically Conductive Concrete for Implementation in Des Moines International Airport," *Case Stud. Constr. Mater.*, 2018, doi: 10.1016/j.cscm.2018.02.003.

[12] S. A. Yehia and C. Y. Tua, "Thin conductive concrete overlay for bridge deck deicing and

anti-icing," *Transp. Res. Rec.*, 2000, doi: 10.3141/1698-07.
[13] M. P. Uysal and M. Z. Sogut, "An integrated research for architecture-based energy management in sustainable airports," *Energy*, 2017, doi: 10.1016/j.energy.2017.05.199.
[14] A. Monsalud, D. Ho, and J. Rakas, "Greenhouse gas emissions mitigation strategies within the airport sustainability evaluation process," *Sustain. Cities Soc.*, 2015, doi: 10.1016/j.scs.2014.08.003.
[15] K. Liu, S. Huang, F. Wang, H. Xie, and X. Lu, "Energy consumption and utilization rate analysis of automatically snow-melting system in infrastructures by thermal simulation and melting experiments," *Cold Reg. Sci. Technol.*, 2017, doi: 10.1016/j.coldregions.2017.03.009.
[16] H. Wang, L. Liu, and Z. Chen, "Experimental investigation of hydronic snow melting process on the inclined pavement," *Cold Reg. Sci. Technol.*, 2010, doi: 10.1016/j.coldregions.2010.04.007.
[17] P. Pan, S. Wu, Y. Xiao, and G. Liu, "A review on hydronic asphalt pavement for energy harvesting and snow melting," *Renewable and Sustainable Energy Reviews*. 2015, doi: 10.1016/j.rser.2015.04.029.
[18] K. Mensah and J. M. Choi, "Review of technologies for snow melting systems," *J. Mech. Sci. Technol.*, 2015, doi: 10.1007/s12206-015-1152-4.
[19] Y. Lai, Y. Liu, and D. Ma, "Automatically melting snow on airport cement concrete pavement with carbon fiber grille," *Cold Reg. Sci. Technol.*, 2014, doi: 10.1016/j.coldregions.2014.03.008.
[20] A. Arabzadeh, H. Ceylan, S. Kim, K. Gopalakrishnan, and A. Sassani, "Fabrication of Polytetrafluoroethylene-Coated Asphalt Concrete Biomimetic Surfaces: A Nanomaterials-Based Pavement Winter Maintenance Approach," 2016, doi: 10.1061/9780784479926.006.
[21] A. Arabzadeh, H. Ceylan, S. Kim, K. Gopalakrishnan, and A. Sassani, "Superhydrophobic coatings on asphalt concrete surfaces: Toward smart solutions for winter pavement maintenance," *Transp. Res. Rec.*, 2016, doi: 10.3141/2551-02.
[22] A. Arabzadeh *et al.*, "Superhydrophobic coatings on Portland cement concrete surfaces," *Constr. Build. Mater.*, 2017, doi: 10.1016/j.conbuildmat.2017.03.012.
[23] C. Chang, M. Ho, G. Song, Y. L. Mo, and H. Li, "Improvement of electrical conductivity in carbon fiber-concrete composites using self consolidating technology," 2010, doi: 10.1061/41096(366)340.
[24] W. Chen and P. Gao, "Performances of electrically conductive concrete with layered stainless steel fibers," 2013, doi: 10.1061/9780784412671.0014.
[25] J. P. Won, C. K. Kim, S. J. Lee, J. H. Lee, and R. W. Kim, "Thermal characteristics of a conductive cement-based composite for a snow-melting heated pavement system," *Compos. Struct.*, 2014, doi: 10.1016/j.compstruct.2014.07.021.
[26] P. J. Tumidajski, P. Xie, M. Arnott, and J. J. Beaudoin, "Overlay current in a conductive concrete snow melting system," *Cem. Concr. Res.*, 2003, doi: 10.1016/S0008-8846(03)00198-4.
[27] A. Sassani *et al.*, "Polyurethane-carbon microfiber composite coating for electrical heating of concrete pavement surfaces," *Heliyon*, 2019, doi: 10.1016/j.heliyon.2019.e02359.
[28] W. Ziegler, "Radiant heating of airport aprons," 2009.
[29] K. Wang, D. E. Nelsen, and W. A. Nixon, "Damaging effects of deicing chemicals on concrete materials," *Cem. Concr. Compos.*, 2006, doi:

10.1016/j.cemconcomp.2005.07.006.
[30] M. Kayama *et al.*, “Effects of deicing salt on the vitality and health of two spruce species, Picea abies Karst., and Picea glehnii Masters planted along roadsides in northern Japan,” *Environ. Pollut.*, 2003, doi: 10.1016/S0269-7491(02)00415-3.
[31] E. L. Thunqvist, “Regional increase of mean chloride concentration in water due to the application of deicing salt,” *Sci. Total Environ.*, 2004, doi: 10.1016/j.scitotenv.2003.11.020.
[32] W. A. Nixon, *Improved Cutting Edges for Ice Removal*. 1993.
[33] R. C. Lee, J. T. Sackos, J. E. Nydahl, and K. M. Pell, “Bridge Heating Using Ground-Source Heat Pipes.,” *Transp. Res. Rec.*, pp. 51–56, 1984.
[34] X. Liu, S. J. Rees, and J. D. Spitler, “Modeling snow melting on heated pavement surfaces. Part I: Model development,” *Appl. Therm. Eng.*, 2007, doi: 10.1016/j.applthermaleng.2006.06.017.
[35] X. Liu, S. J. Rees, and J. D. Spitler, “Modeling snow melting on heated pavement surfaces. Part II: Experimental validation,” *Appl. Therm. Eng.*, 2007, doi: 10.1016/j.applthermaleng.2006.07.029.
[36] X. Liu and J. D. Spitler, “A Simulation Tool for the Hydronic Bridge Snow Melting System,” *12th Int. Road Weather Conf.*, 2004.
[37] X. Liu and J. D. Spitler, “Simulation Based Investigation on the Design of Hydronic Snow Melting System,” *Transp. Res. Board 83rd Annu. Meet.*, 2004.
[38] K. Liu, S. Huang, H. Xie, and F. Wang, “Multi-objective optimization of the design and operation for snow-melting pavement with electric heating pipes,” *Appl. Therm. Eng.*, 2017, doi: 10.1016/j.applthermaleng.2017.05.033.
[39] G. G. Koenig and C. C. Ryerson, “An investigation of infrared deicing through experimentation,” *Cold Reg. Sci. Technol.*, 2011, doi: 10.1016/j.coldregions.2010.03.009.
[40] D. J. Henderson, “Experimental Roadway Heating Project On a Bridge Approach,” no. October, pp. 14–23, 1963, [Online]. Available: http://onlinepubs.trb.org/Onlinepubs/hrr/1963/14/14-002.pdf.
[41] C. Chang, M. Ho, G. Song, Y. L. Mo, and H. Li, “A feasibility study of self-heating concrete utilizing carbon nanofiber heating elements,” *Smart Mater. Struct.*, 2009, doi: 10.1088/0964-1726/18/12/127001.
[42] J. Gomis, O. Galao, V. Gomis, E. Zornoza, and P. Garcés, “Self-heating and deicing conductive cement. Experimental study and modeling,” *Constr. Build. Mater.*, 2015, doi: 10.1016/j.conbuildmat.2014.11.042.
[43] H. Xu, D. Wang, Y. Tan, J. Zhou, and M. Oeser, “Investigation of design alternatives for hydronic snow melting pavement systems in China,” *J. Clean. Prod.*, 2018, doi: 10.1016/j.jclepro.2017.09.262.
[44] C. Y. Tuan, “Roca Spur Bridge: The implementation of an innovative deicing technology,” *J. Cold Reg. Eng.*, 2008, doi: 10.1061/(ASCE)0887-381X(2008)22:1(1).
[45] E. Heymsfield, A. B. Osweiler, R. P. Selvam, and M. Kuss, “Feasibility of Anti-Icing Airfield Pavements Using Conductive Concrete and Renewable Solar Energy,” 2013.
[46] S. Wu, L. Mo, Z. Shui, and Z. Chen, “Investigation of the conductivity of asphalt concrete containing conductive fillers,” *Carbon N. Y.*, 2005, doi: 10.1016/j.carbon.2004.12.033.
[47] Z. Hou, Z. Li, and J. Wang, “Electrical conductivity of the carbon fiber conductive concrete,” *J. Wuhan Univ. Technol. Mater. Sci. Ed.*, 2007, doi: 10.1007/s11595-005-2346-x.

[48] O. Galao, L. Bañón, F. J. Baeza, J. Carmona, and P. Garcés, "Highly conductive carbon fiber reinforced concrete for icing prevention and curing," *Materials (Basel).*, 2016, doi: 10.3390/ma9040281.
[49] M. Sun, Y. Wu, B. Li, and X. Zhang, "Deicing concrete pavement containing carbon black/carbon fiber conductive lightweight concrete composites," 2011, doi: 10.1061/41177(415)84.
[50] M. Hambach, H. Möller, T. Neumann, and D. Volkmer, "Carbon fibre reinforced cement-based composites as smart floor heating materials," *Compos. Part B Eng.*, 2016, doi: 10.1016/j.compositesb.2016.01.043.
[51] C. Y. Tuan, "Electrical resistance heating of conductive concrete containing steel fibers and shavings," *ACI Mater. J.*, 2004, doi: 10.14359/12989.
[52] C. Y. Tuan and S. Yehia, "Evaluation of electrically conductive concrete containing carbon products for deicing," *ACI Mater. J.*, 2004, doi: 10.14359/13362.
[53] J. Deviny, "United States Patent [19]," 1999.
[54] Q. Zhang, Y. Yu, W. Chen, T. Chen, Y. Zhou, and H. Li, "Outdoor experiment of flexible sandwiched graphite-PET sheets based self-snow-thawing pavement," *Cold Reg. Sci. Technol.*, 2016, doi: 10.1016/j.coldregions.2015.10.016.
[55] H. Li, Q. Zhang, and H. Xiao, "Self-deicing road system with a CNFP high-efficiency thermal source and MWCNT/cement-based high-thermal conductive composites," *Cold Reg. Sci. Technol.*, 2013, doi: 10.1016/j.coldregions.2012.10.007.
[56] C. Wang, Z. Fan, C. Shu, and X. Han, "Preparation and performance of conductive tack coat on asphalt pavement," *Constr. Build. Mater.*, 2020, doi: 10.1016/j.conbuildmat.2020.118949.
[57] J. W. Lund, "Pavement snow melting," *Geo-Heat Center, Oregon Inst. Technol.*, 2000.
[58] A. Balbay and M. Esen, "Experimental investigation of using ground source heat pump system for snow melting on pavements and bridge decks," *Sci. Res. Essays*, 2010.
[59] M. S. Kim, D. U. Jang, J. S. Hong, and T. Kim, "Thermal modeling of railroad with installed snow melting system," *Cold Reg. Sci. Technol.*, 2015, doi: 10.1016/j.coldregions.2014.09.010.
[60] H. Zhao, Z. Wu, S. Wang, J. Zheng, and G. Che, "Concrete pavement deicing with carbon fiber heating wires," *Cold Reg. Sci. Technol.*, 2011, doi: 10.1016/j.coldregions.2010.10.010.
[61] T. Yang, Z. J. Yang, M. Singla, G. Song, and Q. Li, "Experimental Study on Carbon Fiber Tape–Based Deicing Technology," *J. Cold Reg. Eng.*, 2012, doi: 10.1061/(asce)cr.1943-5495.0000038.
[62] J. Lai, J. Qiu, J. Chen, H. Fan, and K. Wang, "New Technology and Experimental Study on Snow-Melting Heated Pavement System in Tunnel Portal," *Adv. Mater. Sci. Eng.*, 2015, doi: 10.1155/2015/706536.
[63] K. Zhang, B. Han, and X. Yu, "Nickel particle based electrical resistance heating cementitious composites," *Cold Reg. Sci. Technol.*, 2011, doi: 10.1016/j.coldregions.2011.07.002.
[64] H. M. Zhao, S. G. Wang, Z. M. Wu, and G. J. Che, "Concrete slab installed with carbon fiber heating wire for bridge deck deicing," *J. Transp. Eng.*, 2010, doi: 10.1061/(ASCE)TE.1943-5436.0000117.
[65] W. J. Eugster, "Road and Bridge Heating Using Geothermal Energy, Overview and Examples," *Eur. Geotherm. Congr.*, 2007.

[66] American society of heating refrigerating and air conditioning engineers, *1997 ASHRAE Handbook: Fundamentals*. 1997.
[67] M. Sun, Z. Li, Q. Mao, and D. Shen, "Study on the hole conduction phenomenon in carbon fiber-reinforced concrete," *Cem. Concr. Res.*, 1998, doi: 10.1016/S0008-8846(98)00011-8.
[68] H. W. Whittington, J. McCarter, and M. C. Forde, "The conduction of electricity through concrete," *Mag. Concr. Res.*, 1981, doi: 10.1680/macr.1981.33.114.48.
[69] P. Gu, P. Xie, J. J. Beaudoin, and R. Brousseau, "A.C. impedance spectroscopy (I): A new equivalent circuit model for hydrated portland cement paste," *Cem. Concr. Res.*, 1992, doi: 10.1016/0008-8846(92)90107-7.
[70] P. Xie, P. Gu, and J. J. Beaudoin, "Electrical percolation phenomena in cement composites containing conductive fibres," *J. Mater. Sci.*, 1996, doi: 10.1007/BF00352673.
[71] S. Yehia and C. Y. Tuan, "Bridge Deck Deicing," 1998.
[72] S. Yehia and C. Y. Tuan, "Conductive concrete overlay for bridge deck deicing," *ACI Mater. J.*, 1999, doi: 10.14359/637.
[73] S. Yehia, C. Y. Tuan, D. Ferdon, and B. Chen, "Conductive concrete overlay for bridge deck deicing: Mixture proportioning, optimization, and properties," *ACI Struct. J.*, 2000, doi: 10.14359/821.
[74] D. Derwin, P. Booth, P. Zaleski, W. Marsey, and W. Flood, "Snowfree®, heated pavement system to eliminate icy runways," 2003, doi: 10.4271/2003-01-2145.
[75] T. Wu, R. Huang, M. Chi, and T. Weng, "A study on electrical and thermal properties of conductive concrete," *Comput. Concr.*, 2013, doi: 10.12989/cac.2013.12.3.337.
[76] R. Rao, H. Wang, H. Wang, C. Y. Tuan, and M. Ye, "Models for estimating the thermal properties of electric heating concrete containing steel fiber and graphite," *Compos. Part B Eng.*, 2019, doi: 10.1016/j.compositesb.2018.11.053.
[77] A. Shishegaran, F. Daneshpajoh, H. Taghavizade, and S. Mirvalad, "Developing conductive concrete containing wire rope and steel powder wastes for route deicing," *Constr. Build. Mater.*, 2020, doi: 10.1016/j.conbuildmat.2019.117184.
[78] K. Gopalakrishnan, H. Ceylan, S. Kim, S. Yang, and H. Abdualla, "Electrically conductive mortar characterization for self-heating airfield concrete pavement mix design," *Int. J. Pavement Res. Technol.*, 2015, doi: 10.6135/ijprt.org.tw/2015.8(5).315.
[79] C. Y. Tuan, "Concrete technology today: conductive concrete for bridge deck deicing," vol. 1, no. July, 2004.
[80] S. P. Wu, L. T. Mo, Z. H. Shui, D. X. Xuan, Y. J. Xue, and W. F. Yang, "An improvement in electrical properties of asphalt concrete," *J. Wuhan Univ. Technol. Mater. Sci. Ed.*, 2002, doi: 10.1007/bf02838422.
[81] E. Andreoli *et al.*, "Carbon black instead of multiwall carbon nanotubes for achieving comparable high electrical conductivities in polyurethane-based coatings," *Thin Solid Films*, 2014, doi: 10.1016/j.tsf.2013.11.047.
[82] S. Wen and D. D. L. Chung, "Effects of carbon black on the thermal, mechanical and electrical properties of pitch-matrix composites," *Carbon N. Y.*, 2004, doi: 10.1016/j.carbon.2004.04.005.
[83] B. Huang, X. Chen, and X. Shu, "Effects of electrically conductive additives on laboratory-measured properties of asphalt mixtures," *J. Mater. Civ. Eng.*, 2009, doi: 10.1061/(ASCE)0899-1561(2009)21:10(612).
[84] Á. García, E. Schlangen, M. van de Ven, and Q. Liu, "Electrical conductivity of asphalt

mortar containing conductive fibers and fillers," *Constr. Build. Mater.*, 2009, doi: 10.1016/j.conbuildmat.2009.06.014.
[85] M. J. Khattak, A. Khattab, H. R. Rizvi, and P. Zhang, "The impact of carbon nano-fiber modification on asphalt binder rheology," *Constr. Build. Mater.*, 2012, doi: 10.1016/j.conbuildmat.2011.12.022.
[86] B. O. Lee, W. J. Woo, H. S. Park, H. S. Hahm, J. P. Wu, and M. S. Kim, "Influence of aspect ratio and skin effect on EMI shielding of coating materials fabricated with carbon nanofiber/PVDF," *J. Mater. Sci.*, 2002, doi: 10.1023/A:1014970528482.
[87] J. E. Mates *et al.*, "Durable and flexible graphene composites based on artists' paint for conductive paper applications," *Carbon N. Y.*, 2015, doi: 10.1016/j.carbon.2015.01.056.
[88] A. Das, H. T. Hayvaci, M. K. Tiwari, I. S. Bayer, D. Erricolo, and C. M. Megaridis, "Superhydrophobic and conductive carbon nanofiber/PTFE composite coatings for EMI shielding," *J. Colloid Interface Sci.*, 2011, doi: 10.1016/j.jcis.2010.09.017.
[89] J. Engel, J. Chen, N. Chen, S. Pandya, and C. Liu, "Multi-walled carbon nanotube filled conductive elastomers: Materials and application to micro transducers," 2006, doi: 10.1109/memsys.2006.1627782.
[90] C. Y. Lee, J. H. Bae, T. Y. Kim, S. H. Chang, and S. Y. Kim, "Using silane-functionalized graphene oxides for enhancing the interfacial bonding strength of carbon/epoxy composites," *Compos. Part A Appl. Sci. Manuf.*, 2015, doi: 10.1016/j.compositesa.2015.04.013.
[91] S. Lim, W. Lee, H. Choo, and C. Lee, "Utilization of high carbon fly ash and copper slag in electrically conductive controlled low strength material," *Constr. Build. Mater.*, 2017, doi: 10.1016/j.conbuildmat.2017.09.071.
[92] P. Ahmedzade and B. Sengoz, "Evaluation of steel slag coarse aggregate in hot mix asphalt concrete," *J. Hazard. Mater.*, 2009, doi: 10.1016/j.jhazmat.2008.09.105.
[93] J. Wan, S. Wu, Y. Xiao, Z. Chen, and D. Zhang, "Study on the effective composition of steel slag for asphalt mixture induction heating purpose," *Constr. Build. Mater.*, 2018, doi: 10.1016/j.conbuildmat.2018.05.170.
[94] J. Gao, A. Sha, Z. Wang, Z. Tong, and Z. Liu, "Utilization of steel slag as aggregate in asphalt mixtures for microwave deicing," *J. Clean. Prod.*, 2017, doi: 10.1016/j.jclepro.2017.03.113.
[95] H. Abdualla, H. Ceylan, S. Kim, K. Gopalakrishnan, P. C. Taylor, and Y. Turkan, "System requirements for electrically conductive concrete heated pavements," *Transp. Res. Rec.*, 2016, doi: 10.3141/2569-08.
[96] A. Sassani, H. Ceylan, S. Kim, K. Gopalakrishnan, A. Arabzadeh, and P. C. Taylor, "Influence of mix design variables on engineering properties of carbon fiber-modified electrically conductive concrete," *Constr. Build. Mater.*, 2017, doi: 10.1016/j.conbuildmat.2017.06.172.
[97] N. Banthia, S. Djeridane, and M. Pigeon, "Electrical resistivity of carbon and steel micro-fiber reinforced cements," *Cem. Concr. Res.*, 1992, doi: 10.1016/0008-8846(92)90104-4.
[98] A. S. El-Dieb, M. A. El-Ghareeb, M. A. H. Abdel-Rahman, and E. S. A. Nasr, "Multifunctional electrically conductive concrete using different fillers," *J. Build. Eng.*, 2018, doi: 10.1016/j.jobe.2017.10.012.
[99] X. Fan, D. Fang, M. Sun, and Z. Li, "Piezoresistivity of carbon fiber graphite cement-based composites with CCCW," *J. Wuhan Univ. Technol. Mater. Sci. Ed.*, 2011, doi: 10.1007/s11595-011-0226-0.

[100] M. S. Konsta-Gdoutos and C. A. Aza, “Self sensing carbon nanotube (CNT) and nanofiber (CNF) cementitious composites for real time damage assessment in smart structures,” *Cem. Concr. Compos.*, 2014, doi: 10.1016/j.cemconcomp.2014.07.003.
[101] B. Han, L. Zhang, C. Zhang, Y. Wang, X. Yu, and J. Ou, “Reinforcement effect and mechanism of carbon fibers to mechanical and electrically conductive properties of cement-based materials,” *Constr. Build. Mater.*, 2016, doi: 10.1016/j.conbuildmat.2016.08.063.
[102] S. Jiang *et al.*, “Comparison of compressive strength and electrical resistivity of cementitious composites with different nano- and micro-fillers,” *Arch. Civ. Mech. Eng.*, 2018, doi: 10.1016/j.acme.2017.05.010.
[103] H. Li, H. gang Xiao, and J. ping Ou, “Effect of compressive strain on electrical resistivity of carbon black-filled cement-based composites,” *Cem. Concr. Compos.*, 2006, doi: 10.1016/j.cemconcomp.2006.05.004.
[104] S. Sun *et al.*, “Nano graphite platelets-enabled piezoresistive cementitious composites for structural health monitoring,” *Constr. Build. Mater.*, 2017, doi: 10.1016/j.conbuildmat.2017.01.006.
[105] Y. Ding, Z. Chen, Z. Han, Y. Zhang, and F. Pacheco-Torgal, “Nano-carbon black and carbon fiber as conductive materials for the diagnosing of the damage of concrete beam,” *Constr. Build. Mater.*, 2013, doi: 10.1016/j.conbuildmat.2013.02.010.
[106] A. Al-Dahawi, G. Yıldırım, O. Öztürk, and M. Şahmaran, “Assessment of self-sensing capability of Engineered Cementitious Composites within the elastic and plastic ranges of cyclic flexural loading,” *Constr. Build. Mater.*, 2017, doi: 10.1016/j.conbuildmat.2017.03.236.
[107] G. Yıldırım, M. H. Sarwary, A. Al-Dahawi, O. Öztürk, Ö. Anıl, and M. Şahmaran, “Piezoresistive behavior of CF- and CNT-based reinforced concrete beams subjected to static flexural loading: Shear failure investigation,” *Constr. Build. Mater.*, 2018, doi: 10.1016/j.conbuildmat.2018.02.124.
[108] C. G. Berrocal, K. Hornbostel, M. R. Geiker, I. Löfgren, K. Lundgren, and D. G. Bekas, “Electrical resistivity measurements in steel fibre reinforced cementitious materials,” *Cem. Concr. Compos.*, 2018, doi: 10.1016/j.cemconcomp.2018.03.015.
[109] L. Shi, Y. Lu, and Y. Bai, “Mechanical and Electrical Characterisation of Steel Fiber and Carbon Black Engineered Cementitious Composites,” 2017, doi: 10.1016/j.proeng.2017.04.491.
[110] W. Chuang, P. Lei, L. Bing-liang, G. Ni, Z. Li-ping, and L. Ke-zhi, “Influences of molding processes and different dispersants on the dispersion of chopped carbon fibers in cement matrix,” *Heliyon*, 2018, doi: 10.1016/j.heliyon.2018.e00868.
[111] A. Al-Dahawi, O. Öztürk, F. Emami, G. Yildirim, and M. Şahmaran, “Effect of mixing methods on the electrical properties of cementitious composites incorporating different carbon-based materials,” *Constr. Build. Mater.*, 2016, doi: 10.1016/j.conbuildmat.2015.12.072.
[112] K. M. Liew, M. F. Kai, and L. W. Zhang, “Carbon nanotube reinforced cementitious composites: An overview,” *Composites Part A: Applied Science and Manufacturing*. 2016, doi: 10.1016/j.compositesa.2016.10.020.
[113] B. Zou, S. J. Chen, A. H. Korayem, F. Collins, C. M. Wang, and W. H. Duan, “Effect of ultrasonication energy on engineering properties of carbon nanotube reinforced cement pastes,” *Carbon N. Y.*, 2015, doi: 10.1016/j.carbon.2014.12.094.

[114] L. Wang and F. Aslani, “A review on material design, performance, and practical application of electrically conductive cementitious composites,” *Construction and Building Materials*. 2019, doi: 10.1016/j.conbuildmat.2019.116892.
[115] X. Yu and E. Kwon, “A carbon nanotube/cement composite with piezoresistive properties,” *Smart Mater. Struct.*, 2009, doi: 10.1088/0964-1726/18/5/055010.
[116] B. P. Grady, “Recent developments concerning the dispersion of carbon nanotubes in polymers,” *Macromol. Rapid Commun.*, 2010, doi: 10.1002/marc.200900514.
[117] Y. Jiang, H. Song, and R. Xu, “Research on the dispersion of carbon nanotubes by ultrasonic oscillation, surfactant and centrifugation respectively and fiscal policies for its industrial development,” *Ultrason. Sonochem.*, 2018, doi: 10.1016/j.ultsonch.2018.05.021.
[118] A. Arabzadeh *et al.*, “Influence of Deicing Salts on the Water-Repellency of Portland Cement Concrete Coated with Polytetrafluoroethylene and Polyetheretherketone,” 2017, doi: 10.1061/9780784480946.020.
[119] H. Ceylan, A. Arabzadeh, A. Sassani, S. Kim, and K. Gopalakrishnan, “Innovative Nano-engineered Asphalt Concrete for Ice and Snow Controls in Pavement Systems,” 2017, doi: 10.14311/ee.2016.388.
[120] A. Nahvi *et al.*, “Multi-objective Bayesian optimization of super hydrophobic coatings on asphalt concrete surfaces,” *J. Comput. Des. Eng.*, 2019, doi: 10.1016/j.jcde.2018.11.005.
[121] M. K. Tiwari, I. S. Bayer, G. M. Jursich, T. M. Schutzius, and C. M. Megaridis, “Highly liquid-repellent, large-area, nanostructured poly(vinylidene fluoride)/poly(ethyl 2-cyanoacrylate) composite coatings: Particle filler effects,” *ACS Appl. Mater. Interfaces*, 2010, doi: 10.1021/am900894n.
[122] K. Golovin, M. Boban, J. M. Mabry, and A. Tuteja, “Designing Self-Healing Superhydrophobic Surfaces with Exceptional Mechanical Durability,” *ACS Appl. Mater. Interfaces*, 2017, doi: 10.1021/acsami.6b15491.
[123] L. Lei, L. Zhong, X. Lin, Y. Li, and Z. Xia, “Synthesis and characterization of waterborne polyurethane dispersions with different chain extenders for potential application in waterborne ink,” *Chem. Eng. J.*, 2014, doi: 10.1016/j.cej.2014.05.044.
[124] H. Du *et al.*, “Synthesis and characterization of waterborne polyurethane adhesive from MDI and HDI,” *J. Appl. Polym. Sci.*, 2008, doi: 10.1002/app.28805.
[125] J. Zhao *et al.*, “Synthesis of a waterborne polyurethane-fluorinated emulsion and its hydrophobic properties of coating films,” *Ind. Eng. Chem. Res.*, 2014, doi: 10.1021/ie5040732.
[126] H. Kargarzadeh *et al.*, “Recent developments on nanocellulose reinforced polymer nanocomposites: A review,” *Polymer*. 2017, doi: 10.1016/j.polymer.2017.09.043.
[127] B. Chen, K. Wu, and W. Yao, “Conductivity of carbon fiber reinforced cement-based composites,” *Cem. Concr. Compos.*, 2004, doi: 10.1016/S0958-9465(02)00138-5.
[128] D. D. L. Chung, “Piezoresistive cement-based materials for strain sensing,” *J. Intell. Mater. Syst. Struct.*, 2002, doi: 10.1106/104538902031861.
[129] W. Dong, W. Li, Z. Tao, and K. Wang, “Piezoresistive properties of cement-based sensors: Review and perspective,” *Construction and Building Materials*. 2019, doi: 10.1016/j.conbuildmat.2019.01.081.
[130] A. links open overlay PanelBaoguoHanXunYuJinpingOu, “Chapter 3 - Processing of Self-Sensing Concrete _ Elsevier Enhanced Reader.pdf.” .
[131] A. Al-Dahawi *et al.*, “Electrical percolation threshold of cementitious composites possessing self-sensing functionality incorporating different carbon-based materials,”

Smart Mater. Struct., 2016, doi: 10.1088/0964-1726/25/10/105005.
[132] P. C. Ma, N. A. Siddiqui, G. Marom, and J. K. Kim, "Dispersion and functionalization of carbon nanotubes for polymer-based nanocomposites: A review," *Composites Part A: Applied Science and Manufacturing*. 2010, doi: 10.1016/j.compositesa.2010.07.003.
[133] P. Slobodian, P. Riha, R. Benlikaya, P. Svoboda, and D. Petras, "A flexible multifunctional sensor based on carbon nanotube/polyurethane composite," *IEEE Sensors Journal*, vol. 13, no. 10. pp. 4045–4048, 2013, doi: 10.1109/JSEN.2013.2272098.
[134] N. Xie, X. Shi, D. Feng, B. Kuang, and H. Li, "Percolation backbone structure analysis in electrically conductive carbon fiber reinforced cement composites," *Compos. Part B Eng.*, 2012, doi: 10.1016/j.compositesb.2012.02.032.
[135] H. Chu, Z. Zhang, Y. Liu, and J. Leng, "Silver particles modified carbon nanotube paper/glassfiber reinforced polymer composite material for high temperature infrared stealth camouflage," *Carbon N. Y.*, 2016, doi: 10.1016/j.carbon.2015.11.036.
[136] P. Cong, P. Xu, and S. Chen, "Effects of carbon black on the anti aging, rheological and conductive properties of SBS/asphalt/carbon black composites," *Constr. Build. Mater.*, 2014, doi: 10.1016/j.conbuildmat.2013.11.061.
[137] S. Wen and D. D. L. Chung, "The role of electronic and ionic conduction in the electrical conductivity of carbon fiber reinforced cement," *Carbon N. Y.*, 2006, doi: 10.1016/j.carbon.2006.03.013.
[138] W. Grellmann and S. Seidler, *Polymer Testing*. 2013.
[139] Z. Yang and Q. Wang, "A simple approach to measure the surface resistivity of insulating materials," 2011, doi: 10.1109/IECON.2011.6119630.

BIOGRAPHICAL SKETCH

Mohammad Anis has acquired his bachelor's degree in Civil Engineering from Dhaka University of Engineering and Technology in 2018 and joined the department of Civil Engineering at the University of Texas Rio Grande Valley in Spring 2020 for pursuing a Master's. He worked as a research assistant under Dr. Mohamed Abdel-Raheem and completed his Master of Science in Civil Engineering in December 2021. His research interests are focused pavement design, and transportation engineering. During his Master's, he was awarded the Presidential Graduate Research Assistantship award for all two years. He has published one article in a prestigious conference, another one is accepted. Two journal paper lined up for the submitting stage, one poster presentation, and is on the verge of submitting another article. For pursuing a Ph.D. degree, he is expected to join the Texas A&M University, College Station, Texas in the Civil and Environmental Engineering department. He can be reached at m.anis@duet.ac.bd.